



UNIVERSIDADE DO ALGARVE

Cellulose dissolution and gelation in
alkaline-based solvents

Ana Catarina Dias Pereira

Dissertation

Integrated Master in Biological Engineering

Faro

2020



LUND UNIVERSITY

UNIVERSIDADE DO ALGARVE

Cellulose dissolution and gelation in alkaline-based solvents

Ana Catarina Dias Pereira

Dissertation

Integrated Master in Biological Engineering

Dissertation directed by:

External Supervisor: Prof. Dr. Ulf Olsson

Internal Supervisor: Prof. Dr^a Anabela Romano

Faro

2020

Cellulose dissolution and gelation in alkaline-based solvents

Integrated Master in Biological Engineering

Declaração da Autoria do Trabalho

Declaro ser a autora deste trabalho, que é original e inédito. Autores e trabalhos consultados estão devidamente citados no texto e constam da listagem de referências incluída.

Ana Catarina Dias Pereira

A Universidade do Algarve tem o direito, perpétuo e sem limites geográficos, de arquivar e publicitar este trabalho através de exemplares impressos reproduzidos em papel ou de forma digital, ou por qualquer outro meio conhecido ou que venha a ser inventado, de o divulgar através de repositórios científicos e de admitir a sua cópia e distribuição com objetivos educacionais ou de investigação, não comerciais, desde que seja dado crédito ao autor e editor.

Copyright © 2020 Universidade do Algarve, Portugal

Acknowledgments

First of all, I want to thank Professor Ulf Olsson, my supervisor in Lund University, for accepting me to do my Erasmus+ Internship mobility program at the Physical Chemistry department and for allowing me to be a part of an incredible research group. I appreciate all the support, understanding, teaching, criticism, and patience. Words are not enough to express my gratitude!

A special thanks to my external co-supervisor Dr. Luigi Gentile for his guidance, support and teaching during this research.

I am very thankful for my office colleagues (the best!), for all the support and companionship, you made me feel at home right from the beginning.

I thank everyone in Fkem department for the cheerful and warm environment. My housemates at Möllevångsvägen and friends in Vilhdanden for the fun adventures, interesting discussions and all the good times we had together!

I would like to thank Professor Anabela Romano, my supervisor in Portugal, for giving me this opportunity. For all the help in the bureaucratic process at the University of Algarve, the teaching, and the words of support.

I would like to express my gratitude and appreciation for my internal co-supervisor Dr. Bruno Medronho whose guidance, support and encouragement has been invaluable.

My family, mother, father and sister, for all the love and support. Your belief in me has made this journey possible.

A heartfelt thank you to my late grandmother Herminia and “adoptive” grandparents António and Guilhermina, to whom I dedicate this thesis.

For all this and whatever is to come, thank you all from the bottom of my heart!

Tack så mycket!

Index

Acknowledgments	ii
Index.....	iv
Index for figures.....	vi
Index for tables	viii
List of abbreviations.....	ix
Abstract	xi
Resumo	xiii
1. Introduction.....	1
1.1. Cellulose	3
1.2. Polymers	7
1.3. Solvents	8
1.3.1. Sodium Hydroxide.....	11
1.3.2. Tetra-n-butylammonium hydroxide.....	12
2. Materials and methods	16
2.1. Materials.....	16
2.2. Studied systems	16
2.2.1. Cellulose dissolution in cold Alkali.....	16
2.2.2. Cellulose dissolution in TBAH (aq.).....	17

2.3. Rheology	17
2.3.1. The theory	17
2.3.2. The experiment setup	21
2.4. Wide angle X-ray Scattering.....	22
2.4.1. The technique	22
2.4.2. Experimental setup	24
2.5. Nuclear Magnetic Resonance	24
2.5.1. The theory behind the practice.....	25
2.5.2. The experiment	32
3. Results and discussion	33
3.1. Gelation of cellulose solutions dissolved in NaOH (aq.)	33
3.1.1. Rheometry and turbidimetry	33
3.1.2. Wide angle X-ray Scattering	37
3.2. Solvent interaction with cellulose: role of water, cosolvent and TBA ⁺ cation	40
3.2.1. Self-diffusion NMR	40
4. Conclusion.....	57
5. Future work.....	58
References	59
Appendix A. Pb and graphs.....	71
Appendix B. Published article	73

Index for figures

Figure 1.1.	Schematic of the tree hierarchical structure ¹ . Where ML= middle lamellae between tracheids, P = primary cell wall, S1, S2, S3 = cell wall layers.	4
Figure 1.2.	Chemical structure of cellulose with two β -1,4 linked anhydroglucose units ² .	5
Figure 1.3.	Tetrabutylammonium hydroxide (TBAH) C ₁₆ H ₃₇ NO (adapted from Carl Roth's e-catalogue).	13
Figure 1.4.	Scanning electron microscopy images of the cellulose solutions after being deposited onto a glass lamella followed by solvent evaporation. a): cellulose dissolved in 2 M NaOH aqueous solvent; b): cellulose dissolved in the 1.5M TBAH aqueous solvent. The scale bar represents 5 μ m ³ .	14
Figure 2.1.	Schematic diagram of a concentric bob-and-cup measuring geometry.	19
Figure 2.2.	Schematic representation of response to an oscillatory strain or stress for elastic, viscous, and viscoelastic systems ⁶ .	20
Figure 2.3.	A schematic diagram of a two-site binding model of a ligand (square) with a free diffusion coefficient of D _f (D _{free}), in exchange with a binding site on cellulose. The diffusion coefficient of the bound ligand is D _b , and is taken as being equal to that of the cellulose. Adapted from Price ⁵ .	27
Figure 2.4.	Representation of a PGSE sequence ⁴	28
Figure 3.1.	Loss, G'', (empty circles) and storage, G', (full circles) moduli time dependence at 25.0 °C (a), 27,5 °C (b), 29.5 °C (c) and 30 °C (d).	33
Figure 3.2.	4 wt% cellulose in NaOH (2M) gelation time dependence with temperature	34
Figure 3.3.	Turbidity a) and complex viscosity b) temperature experiments alternating between 25 (black symbols) and 45 °C (grey symbols) for 4 wt% cellulose in NaOH(aq.). Samples were kept for 2 h at each temperature before changing to the other temperature ⁷ .	35
Figure 3.4.	Temperature ramp test in the linear viscoelastic regime at frequency 1 1/s, the temperature was increased with 0.1 °C/min rate from 10 to 40°C (black) and then from 40 to 10°C (grey).	36

Figure 3.5.	Solvent subtracted WAXS-patterns of freshly prepared (dark grey line), aged for 9 h (dark grey line) and aged 144 h (black line) 4 wt% of cellulose in NaOH (aq.) solutions at 45 °C. The arrow highlights the evolution of the main diffraction peak at $q = 1.4 \text{ \AA}^{-1}$.	38
Figure 3.6.	Illustration of the gel structure obtained from cellulose crosslinking where the crystallites are suggested to work as junction points ⁷ .	39
Figure 3.7.	Schematic illustration of the self-diffusion experiments. The sample consists of 4 wt% of cellulose in 40 wt% TBAH/DMSO mixture (1:4 ratio) at 25 °C. The experimental parameters to measure H ₂ O–OH, DMSO and TBA ⁺ self-diffusion coefficients were $D = 140 \text{ ms}$, $d = 2 \text{ ms}$ and g was varied from 0 to 16 g/cm for H ₂ O–OH and from 25.3 to 101.1 g/cm for TBA ⁺ in 16 gradient step.	42
Figure 3.8.	Relative diffusion coefficients of TBA ⁺ (circles), DMSO (triangle) and water (squares) as a function of cellulose concentration in a TBAH/DMSO mixture (1:4 ratio) at 25 °C (grey) and 30 °C (black). Note that a 40 wt. % TBAH (aq.) was used here.	43
Figure 3.9.	Relative diffusion coefficients of TBA ⁺ (circles) and water (squares) as a function of cellulose concentration in a 55 wt% TBAH (aq.) solvent 25°C (grey) and 30°C (black). Note that the solvent used was a 55 wt% TBAH in water.	45
Figure 3.10.	Comparison of the relative diffusion coefficients of TBA ⁺ (circles), DMSO (triangles) and water (squares) as a function of cellulose weight fraction in the solvent system composed by 40wt% TBAH (aq.) and DMSO at 1:1 (red); 1:2 (green); 1:3 (blue) and 1:4 (orange) TBAH/DMSO ratios.	46
Figure 3.11.	Fraction of Pb (a and b) and α values (c and d) of DMSO (squares), TBA ⁺ (circles) and water (triangles) as a function of cellulose weight fraction. The solvent system used is a 40 wt% TBAH (aq.)/DMSO (1:4 ratio) (a and c) and 55 wt% TBAH (b and d) at 25 °C (gray) and 30 °C (black).	48
Figure 3.12.	Summary of fraction of bound molecules of TBA ⁺ and DMSO for 4 weight percent cellulose in solutions of different quantities of TBAH (30%, 40%, 45% and 55%) and different ratios of TBAH (40%) with DMSO at 25 °C and 30 °C.	51

Figure 3.13.	Summary of α values for 4 wt. % cellulose in TBAH solutions of different concentrations (30, 40, 45 and 55 wt. %) and different ratios of 40 wt. % TBAH (aq.) with DMSO at 25°C and 30°C.	53
Figure 3.14.	Summary of α values for 4 wt. % cellulose as a function of the weight fraction of TBAH present in the different solvents used. Green symbols represent the solvents containing DMSO, while the blue symbols represent the systems without DMSO.	54

Index for tables

Table 3.1.	Pb at 4 wt. % cellulose for different solvent systems studied.	50
Table 3.2.	α values obtained through self-diffusion NMR data fittings.....	52

List of abbreviations

AGU	Anhydroglucose
ML	Middle lamellae
P	Primary cell wall
S1, S2, S3	Cell wall layers
C ₆ H ₁₀ O ₅ , n	Glucan units
Da	Dalton
SAXS	Small Angle X-ray scattering
WAXS	Wide Angle X-ray scattering
MCC	Microcrystalline cellulose
NaOH	Sodium hydroxide
TBAH	Tetra-n-butylammonium hydroxide
DMAc	Lithium chloride (LiCl)/N,N-dimethylacetamide
NMP	LiCl/N-methyl-2-pyrrolidone
DMI	LiCl/1,3-dimethyl-2-imidazolidinone
DMSO	Dimethyl sulfoxide
TBAF	Tetrabutylammonium fluoride trihydrate
NMMO	N-methyl-morpholine-N-oxide
LiClO ₄ *3H ₂ O	Lithium Perchlorate Trihydrate
LiSCN*2H ₂ O	Lithium thiocyanate dihydrate
([BMIM]Cl)	1-butyl-3-methylimidazolium chloride
([Amim]Cl)	1-allyl-3-methylimidazolium chloride
CS ₂	Carbon disulfide
IL	Ionic liquids
NOEs	Nuclear Overhauser effects
NMR	Nuclear magnetic resonance
PGSE NMR	Pulsed gradient spin-echo NMR
γ	Strain
σ	Stress

ω	Frequency
ν	Frequency in cycles
δ	Phase angle shift
γ	Deformation
Δt	Time shift
G'	Storage modulus
G''	Loss modulus
θ	Scattering angle
λ	Wavelength
q	Scattering vector
D	Diffusion coefficient
I	Echo amplitude
b	Parameter that is varied experimentally
g	Gradient strength
Δ	Time between gradients
γ	Gyromagnetic ratio of the observed nucleus
δ	Time duration of the gradient
P_b	Fraction of bound molecules
D_{free}	Diffusion coefficient of the unbound molecules
D_b	Diffusion coefficient of the bound molecules
D_{cell}	Diffusion coefficient cellulose
D_0	Diffusion coefficient of TBA+, water and DMSO in the pure solvent.
A	Obstruction factor
α	Average number of reversibly bound molecules
β	Weight fraction of the solvent
T_{gel}	Gelation time
aq	Aqueous

Abstract

Issues of environmental concern and sustainability are pressing for an efficient and growing use of biomass and naturally occurring polymers to create new materials and sustainable opportunities and solutions. An effective utilization and sourcing of cellulose, as the world's most abundant renewable material, not only reduces the consumption of our limited fossil resources but also protects the environment. To produce cellulose based materials for various applications, cellulose requires dissolution at some point, and this task can be challenging. The traditional methods of dissolution have some limitations: some require high investments others create occupational health and environmental issues. Therefore, it is important to develop inexpensive and environmentally "friendly" alternatives to these solvents. With this purpose in mind, the main goal of this work was to study alkaline-based solvents regarding their interaction and effect on cellulose dissolution, while accessing the aggregation and gelation phenomena.

This work was divided in two parts: The first part focus on cellulose dissolution and gelation in sodium hydroxide studied by time resolved rheology, turbidimetry and wide-angle X-ray scattering. The kinetics of gelation are observed to be strongly temperature dependent, changing from several hours down to few seconds when the temperature is increased from 25 to 30 °C. The obtained gels are irreversibly formed.

Wide angle X-ray scattering data reveals the formation of ordered domains, as the sample gels, and it is suggested the gelation is due to the crystallization and precipitation of cellulose. This strongly indicates that the gelation phenomena can be understood as cellulose precipitation/crystallization where an effectively cross-linked network and gelation results from that cellulose chains may participate in more than one crystallite.

This part of the work resulted in a published article that can be found in Appendix B.

The second part focussed on the molecular self-diffusion coefficients measured in cellulose solutions dissolved in 30 wt. %, 55 wt. % and mixtures of 40 wt. % TBAH (aq.)

and DMSO at different ratios, using pulsed field gradient stimulated echo NMR. The results show that dissolution efficiency of TBAH (aq.) is not compromised significantly even when high amounts of the organic co-solvent (DMSO) are present, in agreement with previous studies. Compared with the standard TBAH (aq.) solvent - 55 wt. % TBAH (aq.), the systems with DMSO presented in this work are highly advantageous since they use much less TBAH (substituted by DMSO) making the dissolution process much less expensive and possibly viable for large scale applications.

Additionally, the molecular self-diffusion coefficients obtained highlight that TBAH can “bind” to cellulose within an interval of 0.5 TBA⁺ to 2.3 TBA⁺ per anhydroglucose unit depending on the TBAH amount in solution. The main driving force for this binding may be the favourable electrostatic interactions between the TBA⁺ cations and the deprotonated hydroxyl groups on the cellulose molecules coupled with hydrophobic interactions. Moreover, temperature seems to not have a significant effect on the relative diffusion coefficient of the different species either in the presence or absence of DMSO in the mixture, at least in the temperature range studied.

Keywords: Cellulose; Gelation; NaOH; Crystallites; TBAH; Diffusion.

Resumo

Desde a revolução industrial que a poluição tem sido um problema crescente e, conseqüentemente, o panorama futuro torna-se incerto devido às alterações ambientais e problemas que daí advêm, tais como alterações climáticas, perda de biodiversidade, acidificação dos oceanos, desertificação e a depleção dos recursos aquíferos. Devido a esta realidade, o interesse e motivação para a investigação na utilização eficiente de biomassa e polímeros naturais tem crescido significativamente com o foco no desenvolvimento de novos biomateriais.

O crescente aumento da população gera uma discrepância, cada vez maior, entre oferta e procura de alimentos, materiais, produtos, etc, devido à escassez de área arável e diminuição dos recursos hídricos. No caso dos materiais têxteis, a produção de algodão tem a sua capacidade de produção estagnada, e por isso, procuram-se soluções renováveis e amigas do ambiente que lhe possam servir de alternativa.

Um uso e fornecimento eficiente da celulose não só reduz a necessidade de consumo de recursos fósseis, como protege o planeta a curto e longo prazo. A madeira é a principal fonte de celulose, mas existem alternativas como o linho, cânhamo, sisal, entre outros; a celulose pode ainda ser encontrado em bactérias, algas e fungos.

A celulose é o polímero mais abundante na natureza, com elevada importância económica e variadas aplicações. Graças à sua biocompatibilidade e não toxicidade, a celulose pode ser transformada em diferentes produtos, como fibras têxteis, filmes, espumas, incorporação em formulações alimentares e farmacêuticas, e aplicações biomédicas, entre elas: material de envolvimento para medicamentos, aditivos de produtos farmacêuticos, coagulante do sangue, membranas de rins artificiais, e várias aplicações na engenharia de tecidos e materiais para implantes.

Como a celulose não funde, o seu processamento acarreta a necessidade de dissolução - o que não é tarefa fácil. Apesar de existirem vários solventes para a celulose, a maioria está limitada a usos laboratoriais de pequena escala devido à complexidade dos processos, toxicidade, volatilidade, custos de produção e reciclagem, etc. E por isso, aumenta a necessidade de procurar novos sistemas para a dissolução de celulose e compreender os fundamentos do processo de dissolução (interação soluto solvente) e regeneração. Com o aumento do conhecimento sobre os impactos ambientais e o consequente aumento da regulamentação das indústrias e seus resíduos, a procura por alternativas menos poluentes, mais amigas do ambiente e com processos mais simples, representa uma área de elevado interesse e com cada vez maior importância na indústria.

Neste trabalho foram estudados dois solventes alcalinos. Os solventes estudados foram o hidróxido de sódio (NaOH) e o hidróxido de tetrabutilamónio (TBAH).

O NaOH é um dos solventes mais populares usados na dissolução da celulose. É um sistema relativamente barato, potencialmente não poluente e fácil de aplicar. O intervalo de concentração a que este solvente funciona é pequeno, apenas de 1,5 a 2,5 M e funciona apenas a temperaturas abaixo de zero. Se estas condições não forem cumpridas, a celulose não vai ser dissolvida, apenas absorve solvente (turgência).

Por sua vez, o TBAH é um solvente novo e muito eficiente na dissolução de celulose que tem vindo a ser alvo de vários estudos nos últimos anos. O TBAH é uma solução aquosa de um sal e apesar de ter algumas propriedades comuns aos líquidos iónicos, este tem a particularidade de ser estável em soluções aquosas, o que facilita a sua aplicação.

A adição de DMSO como co-solvente ao TBAH, foi descrita por vários autores como benéfica à dissolução da celulose. O DMSO é um solvente polar que, por si só, não consegue dissolver a celulose, mas como co-solvente já pode participar no processo de dissolução da celulose. Tem a particularidade de atuar como base fraca ou forte, permitindo-lhe dissolver uma vasta gama de substâncias.

O sistema de dissolução TBAH/H₂O/DMSO tem várias propriedades atrativas, tais como a sua estabilidade na presença de água, rápida dissolução e a possibilidade de utilização à temperatura ambiente. No futuro, este sistema parece promissor e poderá vir a ter várias aplicações em equipamentos eletrónicos, ecrãs, tratamentos médicos, entre outros.

Na primeira parte do trabalho, a gelificação de soluções de celulose microcristalina em solventes alcalinos de NaOH (2M), foi acompanhada através de reologia, turbidimetria e de espalhamento de raio-X a ângulo amplo (WAXS), para se compreender a associação das moléculas de celulose e o processo de gelificação. A cinética da gelificação das soluções de celulose é extremamente dependente da temperatura, variando de várias horas para apenas alguns segundos com o aumento da temperatura de 25 °C para 30 °C. Os dados de raio-X indicam a formação de domínios de maior ordem à medida que a amostra gelifica. Isto sugere que a gelificação da celulose pode ser entendida como um processo de precipitação/cristalização, onde a rede reticulada e a gelificação resultam da possível participação das cadeias de celulose em mais do que um domínio cristalino.

A primeira parte do trabalho deu origem a uma publicação que pode encontrada no Appendix B.

Na segunda parte do trabalho, focou-se a análise dos coeficientes de auto-difusão molecular em diferentes soluções de celulose à base de TBAH (aq.) e com DMSO em diferentes rácios. Observou-se que a celulose foi mais facilmente dissolvida em 55% TBAH (aq.) do que em concentrações mais baixas do solvente. Por si só, o 30% TBAH (aq.) não consegue dissolver a celulose, mas surpreendentemente, com a adição de DMSO, foi possível dissolver celulose com quantidades mínimas de TBAH (aq.), ca. 7%, o que torna a dissolução com TBAH mais vantajosa em termos económicos e possivelmente viável para aplicações de maior escala. Os resultados obtidos mostram que o TBAH pode interagir com a celulose, num intervalo de 0.5 iões de TBA⁺ a 2.3 iões de TBA⁺ (em média) por cada unidade de AGU, dependendo da quantidade de TBAH

existente em solução. A principal força motriz desta interação é de natureza eletrostática entre o TBA⁺ e os grupos hidroxilo desprotonados da celulose, sendo espectável ainda a contribuição das interações hidrofóbicas. No intervalo estudado, a temperatura não teve um efeito significativo no coeficiente de difusão das diferentes espécies, tanto na presença como na ausência de DMSO.

Palavras-chave: Celulose; Gelificação; NaOH; Cristalitos; TBAH; Difusão.

1. Introduction

Since the industrial revolution, pollution has been increasing considerably especially the one caused by industrial emissions, vehicular exhausts, and toxic chemicals⁸. Consequently, the long-term outlook remains unclear since our environment is changing and many related problems arising, such as climate change, biodiversity loss, ocean acidification, desertification, and depletion of the world's fresh water supply⁸. Population growth and strong economies are also increasing the resource consumption, and the threat of depletion of non-renewable energy and environmental pollution caused by petroleum-based polymers has been motivating an efficient and growing utilization of biomass and naturally occurring polymers to create new materials and sustainable opportunities and solutions^{9,10}.

Issues of environmental concern and sustainability are increasingly important and gaining more and more space in business and academia as well as in consumers, manufacturers, retailers, and public policy makers decisions^{11,12}. As the financial and intrinsic costs of environmental degradation become clear, sustainability asks that science and technology evolve focussing on natural, renewable and sustainable resources, such as lignocellulose biomass^{12,13}. Therefore, there is an increasing demand of new processes that are intended to be less impactful on the environment and could provide new means to use natural resources in a more efficient manner^{10,12}.

An effective utilization and sourcing of cellulose, not only reduces the consumption of our limited fossil resources but also protects the environment of the Earth, since it is the world's most abundant renewable material, and it is estimated that nearly 700 billion tons are produced every year^{14,15}. With a wide range of beneficial physical and chemical properties, its renewability, biodegradability, biocompatibility, and environmental friendliness, make cellulose very popular in order to produce materials for various applications^{16,17}.

Cellulose in the form of wood pulp is an important renewable resource, and textile fibers based on regenerated cellulose from wood hold great potential^{18,19}. Wood has attracted enormous attention in the preparation of functional materials. It is mainly used for the production of paper (via cellulose extraction), and the other components of wood are mainly incinerated to energy¹⁰. Although it is certainly the most important industrial source of cellulosic fibers, its high demand in different sectors, such as the building products, furniture industries, the pulp and paper industry, as well as the combustion of wood for energy, makes it challenging to supply all users with the quantities needed at reasonable cost²⁰. Some alternative sources for cellulose could be crops such as flax, hemp, sisal, and others, especially by-products of these different plants²⁰.

The demand for textile fibres is constantly increasing, due to the population growth and improving standard of living²¹. Its production is highly dependent on cotton (suffering from severe ecological, environmental and social issues) and synthetic (e.g., nylon, polyester, etc.) based fibers. Therefore, forest/plant based raw materials, as a renewable resource could play a major role in replacing fossil oil-based fibers and cotton by new ecological man-made ones for textiles related products^{14,22}.

Cotton is a very important source of cellulose for textiles, with up to 96% cellulose in its composition, but the demand for sustainable alternatives is increasing not only due to the environmental drawbacks associated with cotton cultivation and processing, such as high water and pesticide usage but also the social issues, such as poor labour conditions, child exploitation, etc²³⁻²⁵. In cotton, the long staple lint produced by ginning the cotton is used for textiles and the shorter, more reactive cotton linters cut from the ginned cotton seed are used for chemical cellulose²³.

The production of cotton and synthetic fibres is not expected to grow significantly in the future, which creates a serious gap between the fibre demand and the production²¹. Candidates to fill the gap are the viscose and the Lyocell processes which produce man-made cellulosic fibres. However, the viscose process is challenging due to the occupational health and environmental issues relating to the use of carbon disulphide²¹. On the other hand, the Lyocell process requires major investments in safety technology

and high solvent recycling to make the all process sustainable¹⁶. As a consequence, there is a need to find (and improve) fibres that are made from the renewable resources (vs. oil), that do not compete with the food production (as cotton) and do not need hazardous chemicals (as viscose) and dangerous processes (Lyocell).

In this work, the main purpose was to study alkaline-based solvents regarding their interaction and effect on cellulose dissolution and the aggregation and gelation phenomena. The results obtained are expected to be quite relevant for the development of alternative sustainable and efficient aqueous-based processes for cellulose man-made textile fiber development or other cellulose-based biomaterials (e.g., films, foams, particles, etc.) from the developed solutions.

1.1. Cellulose

As an important raw material, cellulose has been used since ancient times. It can be obtained mainly from four resources; forestry, agricultural crops, industrial and animal residues, but it can also be found in bacteria, algae and fungi^{16,22}. In cellulose obtained from bacteria, algae and fungi, it is possible to control the production conditions and, consequently, it is possible to control important cellulose properties and the course of biosynthesis (e.g., kinetics, yield and other metabolic products)²².

When the cellulose source is wood, the process starts with dissolving the pulp. Then, as a purified raw material, cellulose is converted by large-scale industrial processing into regenerated materials, such as fibers, films, food casings, membranes, sponges, among others, and new cellulose derivatives, such as esters and ethers that will be used for coatings, films, membranes, building materials, drilling techniques, pharmaceutical formulations, and foodstuffs^{15,22}. Due to its general non-toxicity and good biocompatibility, cellulose and cellulose derivatives are used in medical applications, such as coating materials for drugs, additives of pharmaceutical products, blood coagulant, supports for immobilized enzymes, artificial kidney membranes, stationary phases for optical resolution, in wound care and as implant material and scaffolds in tissue engineering²⁶.

Despite the fact that cellulose is available in any plant, the highest quantity of cellulose is found in the secondary walls of higher plants (Figure 1.1), where the polymer is incorporated in a matrix of lignin, fats, proteins, and shorter heteropolysaccharides, such as hemicelluloses and pectins^{24,27}. As the main compounds, cellulose, lignin and hemicellulose (depending on the source) exist in percentages typically ranging from 40% to 50%, 18% to 35%, and 25% to 35%, respectively^{16,28}. Due to its structural features, cellulose is the most important skeletal component in plants²².

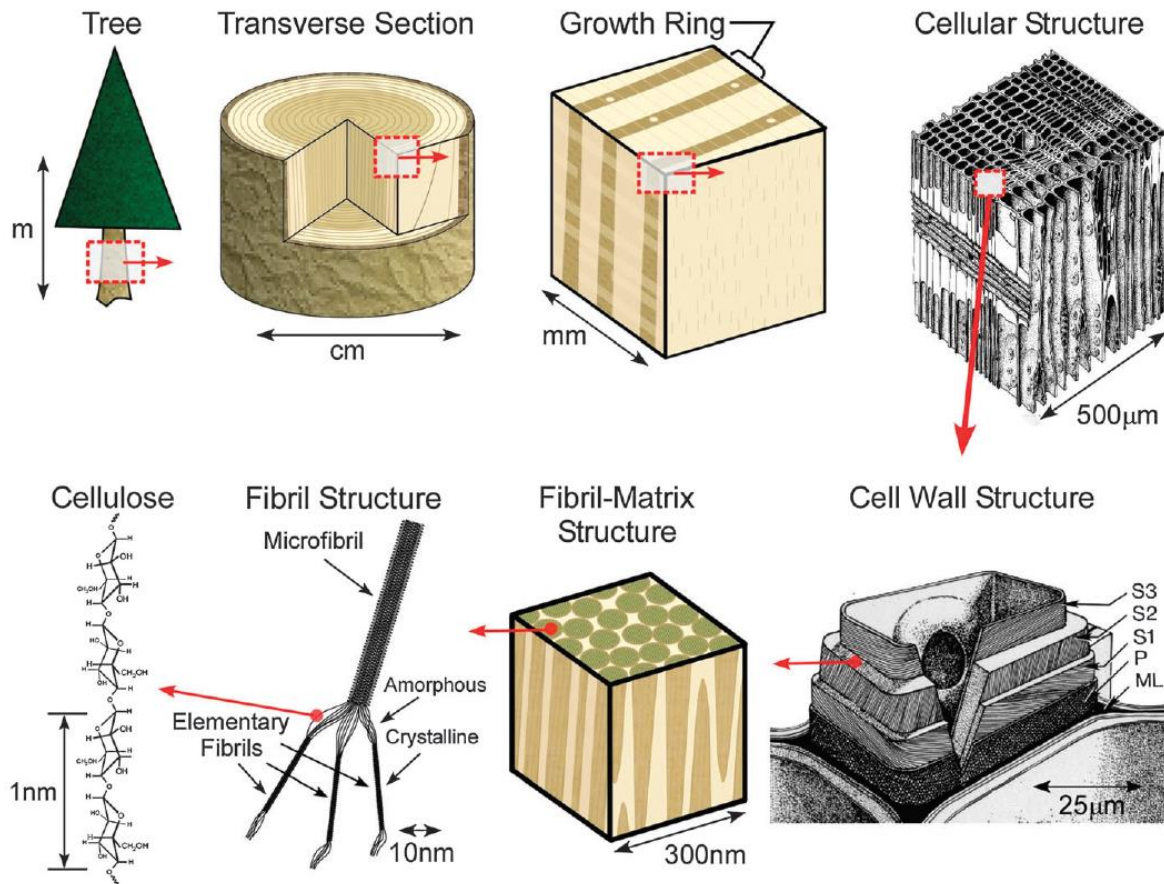


Figure 1.1. Schematic of the tree hierarchical structure¹. Where ML= middle lamellae between tracheids, P = primary cell wall, S1, S2, S3 = cell wall layers.

Native cellulose made by biosynthesis in living organisms is composed only of glucose monomers, as anhydroglucose (AGU) or glucan units ($C_6H_{10}O_5$, n)² (Figure 1.2). In order to form long polymeric units, the monomers are linked in the β -D-(1 \rightarrow 4) configuration with the D-glucopyranosyl units alternating in 180° rotation^{29–33}. This highly functionalized, linear stiff-chain homopolymer is characterized by its hydrophilicity, chirality, biodegradability, broad chemical modifying capacity, and its formation of versatile semicrystalline fiber morphologies²².

These glucosidic linkages permit an extended chain enabling molecular alignment in crystallites (strong microcrystalline regions) and provides reduced solubility²⁹.

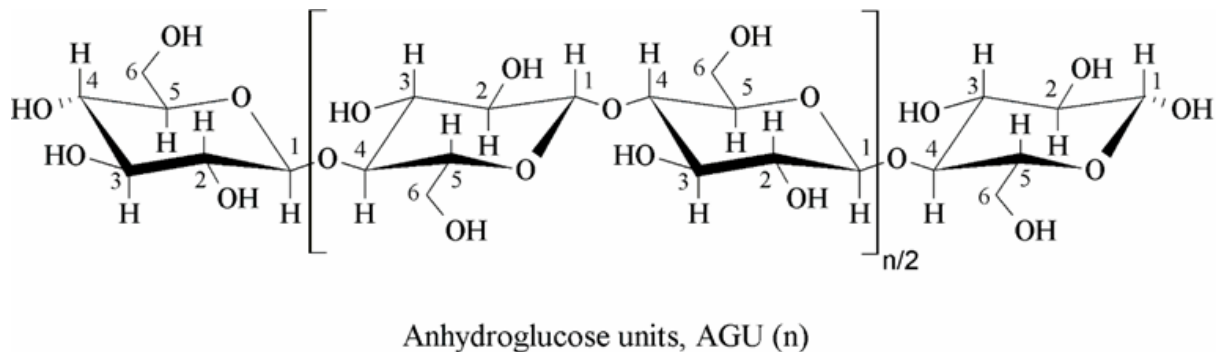


Figure 1.2. Chemical structure of cellulose with two β -1,4 linked anhydroglucose units².

Cellulose is known to exist in the following distinct allomorphs, each with different physicochemical properties: $I\alpha$ (from algae and bacteria), $I\beta$ (from superior plants), II, III_I and III_{II} and IV_I and IV_{II}³⁴. Cellulose I, or native cellulose, is the form found in unprocessed wood and other higher plants^{2,35,36}. Cellulose II is mainly obtained from cellulose I by regeneration (dissolution of cellulose I in a suitable solvent followed by reprecipitation by dilution in water or other nonsolvent)^{2,36,37}. Cellulose III is formed when native cellulose is treated with liquid ammonia at low temperatures, whereas cellulose IV is obtained by treatment of regenerated cellulose at high temperatures³⁴. Each allomorph has structural

variations regarding unit cell dimensions, degree of intra/interchain hydrogen bonding per unit cell and polarity of adjacent cellulose sheets^{2,34}.

Cellulose is a semi-crystalline polymer with amorphous regions, of low order, coexisting with higher order crystalline domains, whose nature arises from strong inter- and intramolecular hydrogen bonding between its monomers^{31,38}. The molecule of cellulose is of intrinsic structural anisotropy with distinctly segregated hydrophilic regions (O-H) and hydrophobic regions (C-H)³⁹. Being quite a polar molecule, it has several -OH groups and thus it has a good hydrogen bonding ability⁴⁰. These groups can form two kinds of hydrogen bonding: inter and intramolecular. The hydrogen intermolecular bonds involve OH groups of neighbour molecules, allowing the formation of a three-dimensional layered structure; while the intramolecular hydrogen bonds, occur between OH groups of the same molecule and provide chain strength and stiffness^{38,41}. Due to its structural anisotropy, cellulose structure, stability and solution behaviour is also affected by other interactions, such as hydrophobic interactions and van der Waals⁴².

In the last years, there has been a discussion on the balance between hydrogen bonding and hydrophobic interactions in controlling the solution behaviour of cellulose^{14,43–45}. The “Lindman hypothesis” asserts that the behaviour and properties of cellulose are significantly influenced and dictated by its amphiphilic character^{40,45}. Such amphiphilicity arises from the above mentioned special segregation of the hydroxyl groups of the anhydroglucose units (equatorial orientation, hydrophilic part), while the C-H bonds have an axial orientation (hydrophobic region)^{46,47}.

Cellulose’s low solubility must have a marked contribution from hydrophobic interactions as well as its extensive intra- and intermolecular bonding^{14,39,48–50}. Since cellulose cannot be melted or easily dissolved in common solvents, the challenge is then to finding efficient and non-degrading solvents^{3,24,31,40,48,51–53}. Among the different solvent systems that are capable of dissolving cellulose, aqueous solutions of strong alkaline agents have shown to be particularly interesting, not only due to their favourable environmental properties but also due to their inexpensiveness and common chemicals used. In this respect, NaOH-based solvents should be highlighted due to its inexpensiveness and low toxicity²⁷.

The cellulose used in this project was microcrystalline cellulose (MCC). MCC is a commercially available material mainly used as a rheological modifier agent and as a binder in the pharmaceutical industry²⁰.

1.2. Polymers

Polymers are macromolecules that consist of repeating structural units, called monomers, connected by covalent chemical bonds⁵⁴. For a polymer, dissolution is typically a slow process controlled by kinetics rather than thermodynamics; the dissolution kinetics becomes slower with higher molecular weight^{55,56}. The molecular weight of polymer molecules may be in the range a few hundreds to millions of Daltons (Da)⁵⁴. Dissolution is controlled by either the disentanglement of the polymer chains and/or by the diffusion of the chains through a boundary layer adjacent to the polymer–solvent interface⁵⁵.

Polymers can be generally classified as either amorphous or semicrystalline. In amorphous systems, crystallization of the polymer chains can be inhibited by steric hindrances by the presence of moieties (branches), cross-links, or by physical entanglements⁵⁷. Polymer chains may be linear or branched⁵⁴.

The crystallization kinetics may affect the polymer microscopic arrangement thus affecting the final material properties^{57,58}. The performance of the polymer is affected by its structure (spatial arrangement of the atoms) and morphology (size, distribution, crystallinity, crystallite, polymer macro-conformation and orientation of crystallites and lamellae), which are strongly affected by processing conditions^{57,58}.

Polymer crystallization is a complex process, where very often the solid phase is only semi-crystalline coexisting with significant amounts of amorphous defects. As for small molecules, polymer crystallization typically goes via a nucleation and growth process. A significant difference between polymer crystallization and the crystallization of small molecules, however, is that polymer chains can participate in more than one nucleus. The

nuclei are often referred to as “fringed micelles” and a cross linked network may arise, leading to gelation (and crystallization) of the system⁵⁹.

To better understand and study polymer crystals or crystals in general, one can use lattice models. The space lattice is a physical model for the crystal structure. It is a three-dimensional infinite array of points, each of which is surrounded in an identical way by its neighbours, and which defines the basic structure of the crystal⁶⁰. The crystal structure consists of a periodic array of identical motifs in three dimensions that will associate with each lattice point an identical structural motif^{60,61}.

X-ray scattering is often used to get information on crystalline phases, estimate size of crystallites, radius of gyration, coil fractal dimension and persistence length. Through Bragg’s law, it is possible to relate the wavelength of the incident X-rays to the glancing angle of reflection⁵⁹.

A polymer with hydrophilic and hydrophobic parts will adjust its conformation in water in order to minimize the free energy (e.g., reduce the contacts between hydrophobic parts and water). However, in the case of a stiff polymer, such as cellulose, these conformational changes are hindered (decrease in conformational entropy), resulting in a decreased solubility in water⁴⁰.

1.3. Solvents

Since cellulose does not melt, dissolution is required to process it in different shapes (e.g., films, sponges, particles, fibers, etc) and new advanced materials. During the last decades, several solvent systems have been developed for manufacturing regenerated cellulose materials and cellulose derivatives¹⁵. Examples of these solvents include lithium chloride (LiCl)/N,N-dimethylacetamide (DMAc), LiCl/N-methyl-2-pyrrolidone (NMP), LiCl/1,3-dimethyl-2-imidazolidinone (DMI), dimethyl sulfoxide (DMSO)/tetrabutylammonium fluoride trihydrate (TBAF), DMSO/paraformaldehyde, N-methyl-morpholine-Noxide (NMMO), aqueous solutions of NaOH and LiOH, some molten salt hydrates, such

as $\text{LiClO}_4 \cdot 3\text{H}_2\text{O}$, and $\text{LiSCN} \cdot 2\text{H}_2\text{O}$, aqueous concentrated salt solutions ZnCl_2 , ammonium, or sodium thiocyanate solutions, aqueous transition-metal complexes (e.g., cuprammonium hydroxide), and ionic liquids such as 1-butyl-3-methylimidazolium chloride ([BMIM]Cl) or 1-allyl-3-methylimidazolium chloride ([Amim]Cl), among others^{15,39,51,62}. However, these solvent systems are mainly limited to a laboratory scale due to different issues, such as dissolving capability, toxicity, high cost of production and/or recovery, uncontrollable side reactions, instability during cellulose processing and/or derivatization, volatility, high energy consumption in solvent recycle, etc^{15,51}.

Ionic liquids are (molten) salts that are liquid below 100° C or even at room temperature⁶³. They are mainly composed of large organic ions, and its bulkiness and mostly very asymmetric structure of the ions prevents crystallization and decreases the melting point⁶³. They have attracted enormous studies in cellulose recently and are considered environment-friendly amphiphilic non-derivatising cellulose I solvents having negligible volatility - which makes them recyclable solvents, and relatively clean manufacturing processes, they seem a promising future towards the achievement of a truly sustainable use of chemicals^{15,47,53,63}. They are non-flammable, high ionic conductivity and have physico-chemical special characteristics, such as adjustable acidity and good solubility towards different solutes^{5,53,64}. However, ionic liquids have some limiting factors, such as high cost of production, high viscosity, sensitivity to moisture content, which can be a problem in large scale processes and poorly developed recovery processes that still need to be improved to make them more economically attractive^{38,65,66}.

The most widely used industrial method for dissolving cellulose in a larger scale is the viscose process, which has been used for more than 100 years⁴⁰. The cellulose-based fibers obtained in this process (Rayon) have excellent properties for a wide range of products from wet-strength cotton-like textile fibers to technical fibers, as the cord in high-performance tires¹⁵. In this system, NaOH is used to swell cellulose pulp, which is then reacted with CS_2 to yield a cellulose derivative that is soluble in the alkaline aqueous solution⁶⁷. Cellulose is then regenerated in sulfuric acid aqueous solutions to shape fibers⁴⁰. This process is technologically complex, and far from being environmentally

friendly due to the use of CS₂, heavy metal compounds (in the precipitation process), and by-products^{15,68}. In addition, the unpleasant scent from CS₂ even at the highest dilution and its toxicity have triggered scientists to search for alternatives in fabricating regenerated cellulose man-made fibers⁶⁷. Despite the environmental concerns, since it is a relatively inexpensive process, it continues to be the main method used worldwide for the regenerated cellulose fiber production, with ca. 4.9 million tons produced globally in 2013⁶⁹.

A new technology was introduced into the market during the 1980s and uses direct dissolution of cellulose to produce lyocell fibers¹⁶. In this “greener” process, cellulose is dissolved at high temperatures (90 °C) and the key ingredient, N-methylmorpholine-N-oxide (NMMO), in combination with water can dissolve cellulose without prior activation or derivatization. The dissolved dope can then be placed in the aqueous nonsolvent medium where cellulose precipitates almost instantaneously^{22,51}. In this process, there is no chemical reaction involved and no chemical by-products are formed. Therefore, it is considered a fairly environmentally friendly process¹⁵. Nevertheless, this system is restricted to a small operating window in which the dissolution parameters are optimal and this constitutes a major limitation⁵¹. In a closed system, NMMO is recovered from the precipitation bath in high yields ranging from 99.6-99.7%^{22,67,69}. Despite the many advantages presented by the lyocell process, it did not replace viscose approach, since lyocell requires high temperature to dissolve cellulose which may degrade it, the side reactions of the solvent itself without antioxidants, its high cost of production (only viable if the solvent is efficiently recycled), as well as major investments in safety technology due to solvent instabilities^{15,16,22,40}.

As result of the increasing environmental consequences awareness, governments are increasing regulations in industries, and the need to develop inexpensive and environmentally “friendly” alternatives to the polluting solvents is thus of great interest and increasingly important to the industries^{3,15}.

1.3.1. Sodium Hydroxide

One of the most popular solvents is NaOH, which has been widely used. This system is inexpensive, potentially non-polluting, uses very common chemicals and relatively easy to handle⁴³. The concentration range in which NaOH works as a direct solvent is very narrow^{27,38,48,70}, ranging from 1.5 to 2.5 M and only at lower temperatures⁷¹.

Therefore, the conditions for cellulose dissolution in NaOH (aq.) must be rigorously controlled, since the concentration range is very small, and the temperature must be below zero. If these conditions are not met, cellulose will not dissolve and will only swell. One of the leading opinions today regarding the dissolution mechanism in cold alkali is that NaOH and water create a hydrate that is able to break the intra- and intermolecular hydrogen bond network between the cellulose molecules^{55,72}.

In this thesis, the NaOH/H₂O system was used to understand the gelation and aggregation phenomena in cellulose solutions. Understanding the way cellulose is organized during gelation and which structures are formed is very important to develop materials with better properties, and it may also provide important hints regarding the dissolution mechanism, which is still not fully understood. These solutions start as clear and fluid, and while some samples are quite stable, others undergo gelation easily. The gelation occurs either with temperature, changes in solvent quality (i.e., pH, ionic strength, additives, dilution, etc), or time^{7,38,60,70,72–74}. The effect of temperature in cellulose based solution dissolved in cold alkali has been studied by Roy et al., and it well established that that the solution's stability is strongly temperature dependent^{70,71}.

Rheological studies of the cellulose system can give further physical insight into the microstructure of the complex polymeric network. Despite the time resolved rheological measurements of the linear viscoelastic properties of cellulose solutions in 2.2 M NaOH(aq.) in the temperature range 15–35 °C performed by Roy et al. in 2003, the reason for the system's gelation was not clarified, and has since not yet been fully explained⁶³.

As mentioned, these mixtures are strongly temperature dependent. The gelation time (T_{gel}) can be estimated from the storage, G' , and loss, G'' , moduli crossover, with increasing temperature^{7,70,72}. Similar results have been reported by Weng et al. in NaOH/thiourea based system⁷⁵. The gelation in alkali is thermo-irreversible; once formed, the gel will not return to the liquid state regardless the temperature performed⁷². The gelation time is also affected by the cellulose concentration; the higher the cellulose concentration, the faster the gelation kinetics.

1.3.2. Tetra-n-butylammonium hydroxide

Recent studies have highlighted onium hydroxides, such as tetra-n-butylammonium hydroxide (TBAH) as very interesting solvent systems with high capacity of dissolving cellulose, other biopolymers and carbohydrates to a large extent, as well as lignin from different wood samples under relatively mild conditions^{51,53,65,71,76–78}. In addition, these systems have been used to successfully dissolve wood (up to a certain wood concentration)¹⁰.

Onium hydroxides, similarly to ionic liquids, are mainly composed of large organic ions, and its bulkiness and mostly very asymmetric structure of the ions prevents crystallization and decreases the melting point⁶³; but unlike ionic liquids, are usually aqueous solutions and have the capability to dissolve wet cellulose I samples⁴⁷. These solvents are liquid at room temperature, are less viscous than IL and do not require high temperatures to dissolve cellulose. This system is a highly basic, low-viscous solvent that has been reported as a new dissolution medium that can dissolve up to 25% cellulose at room temperature^{39,76,79}.

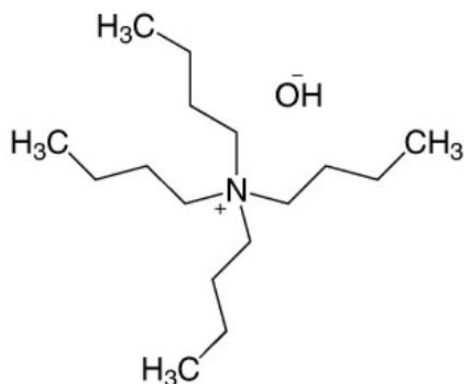


Figure 1.3. Tetrabutylammonium hydroxide (TBAH) C₁₆H₃₇NO (adapted from Carl Roth's e-catalogue).

Cellulose is soluble in TBAH-based solutions because these systems are said to break the intra- and intermolecular hydrogen bonds⁴⁰. The evident amphiphilic properties of the cation are also expected to help the dissolution of an amphiphilic molecule, such as cellulose. In fact, solutions of organic acids or bases are superior solvents to those of inorganic ones⁶⁰. For instance, cellulose dissolution in TBAH is observed to proceed down to the molecular level, while NaOH does not dissolve cellulose molecularly; it rather leaves aggregates of high crystallinity stable in the cellulose dope^{3,7} (Figure 1.4).

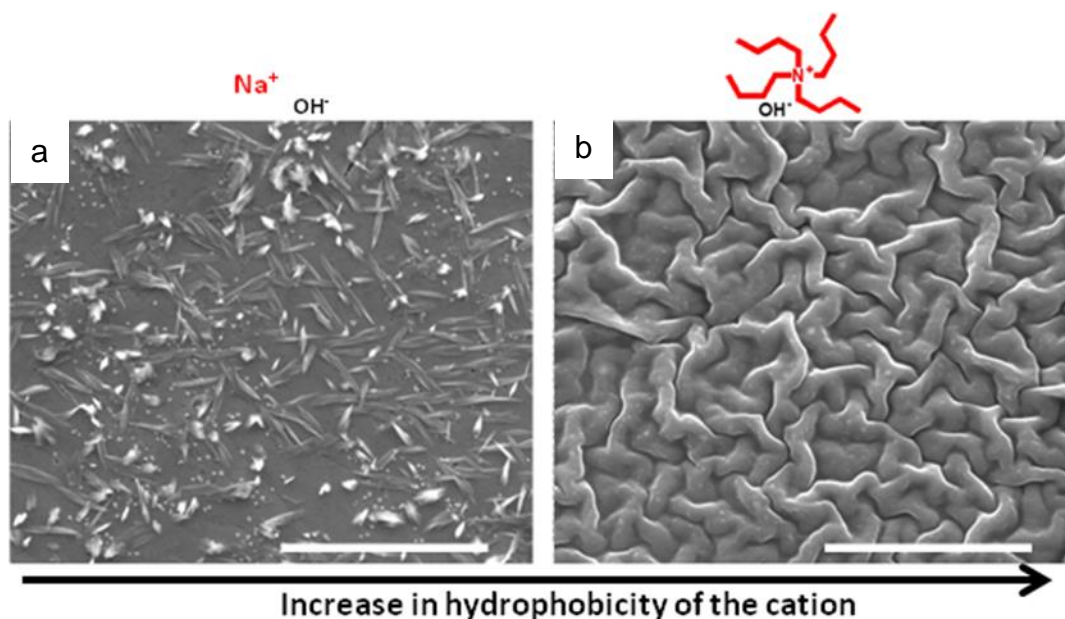


Figure 1.4. Scanning electron microscopy images of the cellulose solutions after being deposited onto a glass lamella followed by solvent evaporation. a): cellulose dissolved in 2 M NaOH aqueous solvent; b): cellulose dissolved in the 1.5M TBAH aqueous solvent. The scale bar represents 5 μm^3 .

It was inferred that 1.2 TBA⁺ ions bind per AGU unit and this was later supported by detailed scattering studies where the SAXS data suggests the presence of a solvation shell enriched in TBA⁺ ions around the cellulose molecules⁸⁰. The TBA⁺ cation is suggested to interact by electrostatic interactions with the (partially) deprotonated hydroxyl groups of cellulose, in addition to hydrophobic interactions due to its amphiphilicity⁸¹. Furthermore, cellulose solubility has been observed to increase as a function of increasing cation hydrophobicity⁸².

In this work, cellulose was dissolved in different weight fractions of TBAH at different temperatures, with and without the addition of dimethyl sulfoxide (DMSO). With this solvent mixture, natural cellulose dissolves in an easy and fast way under mild conditions (i.e., room temperature and atmospheric pressure)⁸³. As observed by Cao et al., adding DMSO into TBAH (aq.) solvent system, one can promote the dissolving capability of the

natural cellulose⁸³. DMSO is an excellent cosolvent and one of the best-known swelling agents for cellulose.

The properties of the different cellulose solution were also accessed through nuclear magnetic resonance (NMR) spectroscopy in order to get detailed information about solvent-cellulose interactions⁶³.

Diffusion NMR can provide information on whether two molecules are bound to each other in a single diffusion experiment. However, by performing a series of measurements, at different concentrations, one can determine the binding constant⁵. This approach was applied to the TBAH-DMSO-cellulose mixtures. The diffusion data was obtained from Pulsed Gradient Spin Echo (PGSE) NMR diffusion measurements, where samples are placed in a strong magnetic field and irradiated with radiofrequency radiation and then recast in terms of the average molecular weight using the Stokes-Einstein equation^{5,84}.

In this experimental setup, Diffusion NMR spectroscopy was used to follow the diffusion coefficients of the solvent species as a function of cellulose concentration⁸⁵.

2. Materials and methods

2.1. Materials

MCC - Avicell PH-101, with a degree of polymerization of 260 and an average particle size of 50 μm was purchased from Sigma-Aldrich. NaOH anhydrous pellets (97% pure), were purchased from Merck and EKA. TBAH (aq.), of chromatographic grade was purchased as 40 wt. % and 55 wt.% aqueous solutions from Sigma-Aldrich. The water used was purified in-house using a MILLIPORE Milli-Q Gradient A10, Millipore, Molsheim, France.

2.2. Studied systems

2.2.1. Cellulose dissolution in cold Alkali

The cellulose solutions in alkali were prepared as described elsewhere^{70,71}. Briefly, 4 wt.% MCC was added to freshly prepared NaOH stock solutions (2M). When cellulose was observed to be well dispersed, the solutions presented a milky aspect. The vials were then placed in ice under stirring for about 10 minutes. At this stage, the solutions become more transparent. Next, the samples were placed in a freezer for 3 hours. Finally, after the freezing step, the solutions were allowed to slowly thaw at 10 °C under constant stirring for, at least, 10 minutes. A viscous and transparent dope was obtained indicating the successful cellulose dissolution.

2.2.2. Cellulose dissolution in TBAH (aq.).

In order to prevent clumping and sedimentation, the cellulose solutions using the TBAH (aq.) as the solvent, were prepared by weighing different amounts of cellulose and slowly adding them to the TBAH (aq.) solutions under vigorous stirring in an ARE stirrer made by VELP Scientifica. A similar procedure was performed when using DMSO as a co-solvent. In this case, different TBAH/DMSO ratios were firstly prepared before adding the desired amount of cellulose. Cellulose concentrations ranging from 0.1 wt.% up to 6 wt.% were dissolved in TBAH (aq.) with solvent concentrations ranging from 30% up to 55 wt% TBAH (aq.). A 40 wt% TBAH (aq.) commercial solution was used to prepare the mixture with DMSO in different ratios (i.e., 1:1, 1:2, 1:3 and 1:4). Samples were kept stirring at room temperature until fully dissolved. The dissolution state was verified periodically under polarized light in an optical microscope. When ready, the samples were either loaded into a nuclear magnetic resonance (NMR) capillary and transferred to a 200MHz NMR spectrometer, Bruker Avance DMX200 spectrometer or alternatively analysed in a mechanical rheometer.

2.3. Rheology

2.3.1. The theory

Rheology is the science that studies the deformation of matter under the influence of an external force^{86,87}. It comes from the Greek word “rheo”, which means flow.

Rheological studies are considered a useful tool for physical characterization in most areas requiring product formulation. Its use goes from raw materials and processing, to intermediate products during manufacturing and finished goods, as well as storage, transportation and product performance⁸⁸. It is important in, for instance, the manufacture and applications of plastic materials, lubricating materials, coatings, inks, adhesives, food,

pharmaceuticals, cosmetics, toiletries, liquid detergents and agrochemical formulations⁸⁹.

Rheometry is the mechanical spectrometry which may provide direct or indirectly structural information of matter and address questions, such as how it is built, what is its molecular structure and morphology, etc. Rheometry can indirectly provide hints on molecular association, their size and structure type (needle or bulky)⁹⁰.

Rheometry is important to study substances with complex behaviour, attempting to establish a relationship between the stress (mechanical force) acting on a given material and the resulting deformation and flow of matter that takes place^{88,91}. The deformation will depend on the state of matter; gases and liquids often display an irreversible (viscous) flow when a force is applied, whilst solids will respond in a reversible (elastic) way being deformed by a fixed amount. The pure solid material is expected to regain its shape when the force is removed^{86,91-93}. In the viscous process, energy is dissipated and in the elastic process energy is stored and released⁹¹. Few materials behave as either perfect elastic solids or perfect viscous liquids. Most of the substances show both viscous and elastic behaviour, the so called viscoelastic behaviour⁹⁴.

From an experimental point of view, the rheological measurements can be carried out on three main geometries, namely the concentric cylinder (Couette), the cone-and-plate and the parallel plate-plate configuration⁹⁵.

Our experiments were carried out on a concentric cylinder, that consists of an inner (bob) and outer (cup) (figure 2.1), which is the most convenient geometry for low viscous liquid-like samples, mainly due to its high sensitivity (high surface area), capability of applying low torques (stress) or oscillation at a variety of amplitudes and frequencies and minimum sample evaporation when using a proper solvent trap^{7,95}.

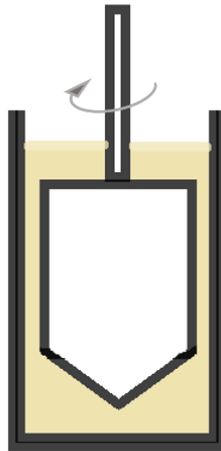


Figure 2.1. Schematic diagram of a concentric bob-and-cup measuring geometry.

Experiments can be performed in a non-linear (rotational tests) or linear (oscillatory tests) fashion. In the latter case, a sinusoidal strain γ or stress σ is applied at a frequency ω (rad s^{-1}), where $\omega = 2\pi v$, and v is the frequency in cycles s^{-1} or Hz ⁶.

After an initial period of applying a certain strain there will be a stress response, which will oscillate with the same frequency. The sign waves of strain and stress (or vice versa) are compared in order to obtain the phase angle shift, δ ⁹⁵. The change of the sine waves of the stress and strain with time can be analysed to distinguish between elastic, viscous, and viscoelastic responses⁶:

- **Perfectly elastic solids will have $\delta = 0$** , when the maximum of the stress amplitude is at the same position as the maximum of the strain amplitude there will be no time shift between the stress and strain sine waves.
- **Perfectly viscous liquid $\delta = 90^\circ$** , occurs when the maximum of the stress is at the point of maximum shear rate where there is maximum energy dissipation. Here the strain and stress sine waves are shifted by $\omega t = \pi/2$.
- **Viscoelastic system $0 < \delta < 90^\circ$** , here, the phase angle shift δ is greater than 0° but less than 90° .

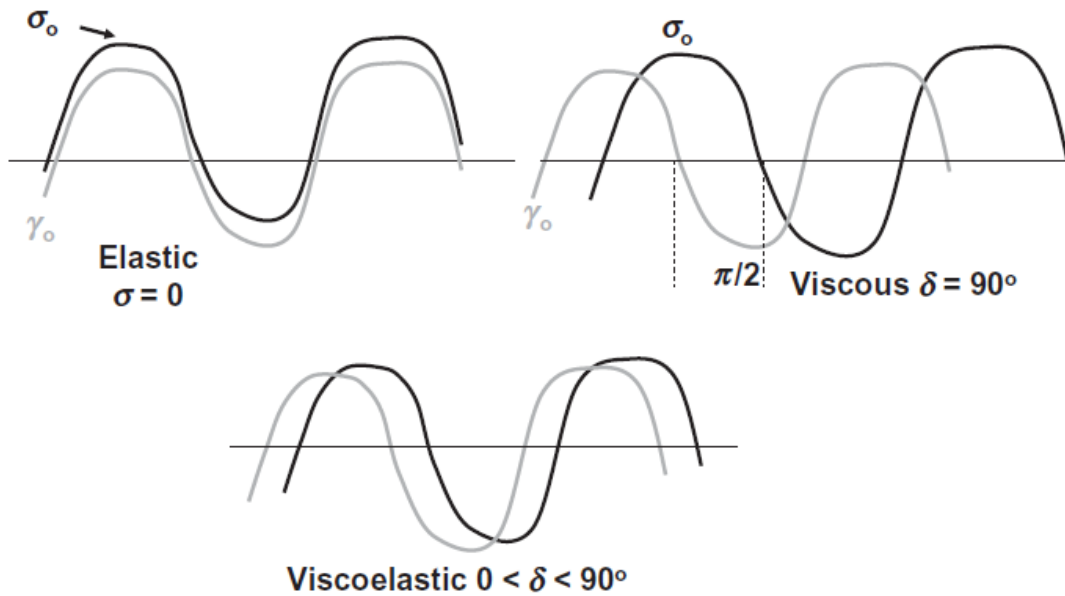


Figure 2.2. Schematic representation of response to an oscillatory strain or stress for elastic, viscous, and viscoelastic systems⁶.

The stress is given by the equation (2.1) while the deformation γ is obtained from eq. 2.2, phase angle shift δ is represented in eq. 2.3, where Δt is the time shift for sine waves of stress and strain:

$$\sigma = \sigma_0 \cos \omega t \quad (2.1)$$

$$\gamma = \gamma_0 (\cos \omega t - \delta) \quad (2.2)$$

$$\delta = \omega \Delta t \quad (2.3)$$

From equation (2.4) and (2.5) one can calculate the storage modulus G' (the elastic component) and the loss modulus G'' (the viscous component), from σ_0 , γ_0 and δ ⁹⁵:

$$G' = \frac{\sigma_0}{\gamma_0} \cos \delta \quad (2.4)$$

$$G'' = \frac{\sigma_0}{\gamma_0} \sin\delta \quad (2.5)$$

Where G' is the elastic component (storage modulus), while G'' is the viscous component (loss modulus).

Typically, the “gel” or “liquid” properties of a certain material can be identified via the behaviour of G' and G'' ⁹⁶. When in the presence of an ideal elastic gel, G' is expected to be frequency-independent and greater than G'' ^{86,92,96,97}. On the other hand, if G'' is bigger than G' , the liquid-like behaviour prevails⁹⁴.

The rheological parameters obtained as a function of amplitude and frequency can be analysed with a variety of models⁹⁵.

2.3.2. The experiment setup

2.3.2.1. Gelation time

Rheological experiments were performed in a stress controlled Anton Paar Physica MCR 301 rheometer, with direct strain oscillation for real-time strain control in a couette cylinder geometry measuring cup (cup diameter: 28.929 mm, bob diameter: 26.673 mm, bob length: 39.997 mm) with 1mm gap and a Peltier heating unit. After loading the sample in the rheometer geometry at 10 °C, temperature was increased to the desired value. In order to minimize the effect of solvent evaporation, a solvent trap was used to cover the sample.

The influence of temperature on the gelation process of the 4 wt.% cellulose dissolved in 8 wt. % NaOH (2M NaOH) aqueous solution was studied by measuring the time evolution of the dynamic moduli (G' and G'') at different temperatures from 25 to 30 °C at $\omega = 1$

rad/s and a constant strain $\gamma = 0.1$. The strain value was selected after amplitude sweep experiments, where the linear viscoelastic regime was inferred.

In the amplitude sweep, the strain was increased from 0.01 to 100%, while the strain was kept constant at 1 rad/s.

2.3.2.2. Temperature ramp tests and frequency sweeps

In order to characterize the material, a sequence of five tests was performed. Firstly, a frequency sweep test was performed at 10 °C with a $\gamma = 0.1$ % and a ω ranging from 0.1 to 100 rad/s, to characterize the solution after it was loaded in the rheometer. This test was followed by a temperature ramp test with increasing temperature from 10 °C to 40 °C at different heating rates, with a $\gamma = 0.1$ % and a constant ω of 1 rad/s, to observe the transition temperature as a function of the temperature rate. A third experiment consisting in another frequency sweep was performed with the same strain and angular frequency as the first frequency sweep test at 40 °C aiming to verify the sample state after the temperature ramp. Next, this test was followed by another temperature ramp, where the temperature was decreased from 40 °C to 10 °C at different rates to see if the transition was reversible. Lastly, another frequency sweep test was done in order to compare with the initial state after loading the sample.

2.4. Wide angle X-ray Scattering

2.4.1. The technique

X-ray diffraction (XRD) techniques are commonly used in the characterization of the structure and morphology of polymers and polymer composites⁵⁷. While wide-angle X-ray scattering (WAXS) is used on atomic and molecular structures to determine the crystal structure, disorder degree and molecular orientation, small-angle X-ray scattering (SAXS)

is suitable to investigate the structure on larger length scales, accessing different information, such as the radius of gyration, coil fractal dimension and persistence length.^{57,59}

Generally speaking, the X-ray diffraction methods rely on Bragg's law which relates the glancing angle of incidence of x-rays and the separation lattice planes⁶⁰.

At a particular angle, θ , with respect to the direction of the primary beam of X-rays, the radiation will constructively interfere to produce intensity maxima based on the wavelength and the geometry and spacing between atoms in the lattice⁹⁸. This is reflected in the Bragg equation (eq. 2.7), where d is the lattice spacing in one of the crystallographic planes.

Typically, the diffracted intensities are recorded as a function of the scattering vector (or momentum transfer) q , which is related to the scattering angle 2θ by the relation 2.6, where λ is the wavelength of the incoming light and θ is the scattering angle:

$$q = \frac{4\pi}{\lambda} \sin \frac{\theta}{2} \quad (2.6)$$

When coherently scattered X-rays from atoms in neighbouring planes interfere with each other, then Bragg's law holds:

$$n\lambda = 2d \sin \theta \quad \text{or} \quad d = \frac{2\pi}{q} \quad (2.7)$$

with d as the lattice spacing in the crystallographic plane and n as an integer number. For a given wavelength, the smaller the separation d of the layers, the greater the scattering angle (so that $2d \sin\theta$ remains constant)⁶⁰.

2.4.2. Experimental setup

Wide-angle X-ray scattering measurements were performed using the SAXSLab Ganesha 300XL instrument (SAXSLAB ApS, Skovlunde, Denmark), a pinhole collimated system equipped with a Genix 3D X-ray source (Xenocs SA, Sassenage, France). Data were collected with the detector placed at a sample-to-detector positions that yields to the WAXS region between 0.5 and 2.5 Å⁻¹. The sample was sealed in the capillary (1.5 mm diameter) and measured “fresh” and after 9 and 144 hours at 45 °C. During the experiments, the temperature was controlled by an external recirculating water bath with an accuracy of 0.2 °C. The two-dimensional (2D) scattering pattern was recorded using a 2D 300 k Pilatus detector (Dectris Ltd., Baden, Switzerland) and radially averaged using SAXSGui software to obtain I(q). The measured scattering curves were corrected for solvent scattering.

2.5. Nuclear Magnetic Resonance

2.5.1. The basics

Nuclear magnetic resonance deals with the interaction between radiofrequency electromagnetic radiation and atomic nuclei in a magnetic field^{63,99}. Modern NMR spectroscopy of liquids provides information on properties, such as chemical shifts, nuclear Overhauser effects (NOEs), relaxation rates, nuclear quadrupole coupling constants or self-diffusion coefficients¹⁰⁰. In diffusion-NMR, the PGSE approach is often used. This methodology is non-invasive and directly probes the dynamics of a system by measuring diffusion^{5,99,101}. It has an important role to play in clarifying mechanisms, especially since it allows the translational motion of all of the species present to be

studied⁵. This technique combines other bulk properties, such as viscosity, density, and electrical conductivity, providing a thorough understanding of molecular transport in ILs¹⁰². Along with other advantages, this is a very convenient and powerful method which typically requires short experiment time, high sensitivity and accuracy providing detailed molecular resolution without the need for adding external potentially perturbing probes or chemically introducing isotopes^{63,99}.

2.5.1. The theory behind the practice

Self-diffusion, also known as intra-diffusion (or translational displacements), is the motion of particles due to the Brownian motion where the diffusion coefficient D , is a measure of the diffusion^{63,103,104}. This can be obtained by PGSE principles¹⁰³.

In this study, PGSE NMR experiments were used to investigate the solvent-solute interactions and determinate the effect of DMSO as a co-solvent in the dissolution of cellulose⁵⁰.

The experiment was carried out by varying the gradient strength while keeping the time variables constant and recording the NMR signal I , the echo amplitude, as a function of b ^{50,63}.

I is given by

$$I = I_0 e^{-bD} \quad (2.8)$$

where I_0 is the amplitude in the absence of field gradients, or static magnetic field, and D is the diffusion coefficient, which is the proportionality between flux and concentration gradient^{50,63,105}.

The parameter b , which is the diffusion-weighting variable, which is varied experimentally is given by¹⁰⁶

$$b = \gamma^2 \delta^2 g^2 \left(\Delta - \frac{\delta}{3} \right) \quad (2.9)$$

Here, g stands for the gradient strength, γ is the gyromagnetic ratio of the observed nucleus (constant for each nucleus), δ is the time duration of the gradient and Δ represents the time between gradients and corresponds to the observations time of the molecular translational diffusion¹⁰⁷. Different gradient values are applied as a function of time, slightly changing the position of the spin. Thus, the gradient serves as a marker by spatially labelling the molecules^{4,50,63,108,109}

In PGSE (figure 2.3) is represented the pulse sequence used, in which two equal gradient pulses of duration δ and direction and magnitude g are inserted into each τ period. δ is typically in the range of 1 – 10 ms, and the separation Δ between the leading edges of the gradient pulses is normally in the range of 10 ms to 1 s^{4,5,106}. The second half of the echo is used as the NMR signal^{4,5}.

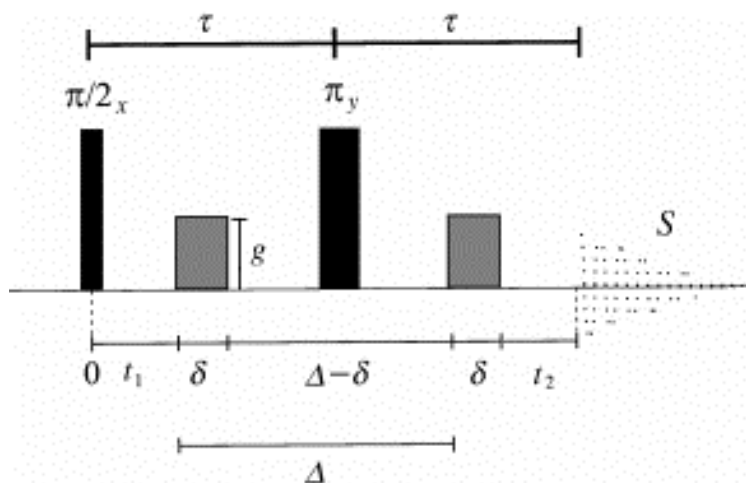


Figure 2.3. Representation of a PGSE sequence⁴.

Experiments were performed at fixed δ and Δ , varying g . Circa 16 different g values were used to measure the echo decays. The diffusion coefficient was extracted by least-squares fitting to the measured diffusion decay points¹⁰⁷.

The diffusion coefficient value will depend on the characteristics of the molecules of interest, on the solvent and the temperature¹¹⁰. The diffusion of the solvent molecules can be affected by the presence of cellulose and vice-versa. Cellulose acts as an excluded volume for the solvent molecules and in this way obstruct their diffusion paths. This obstruction effect is, however, small¹¹¹.

If solvent molecules reversibly associate or bind to cellulose, they will diffuse together with cellulose and present a lower diffusion coefficient. In the case of water, we need to consider that we are measuring the diffusion of protons. The $-OH$ protons exchange fast between the three different sites: H_2O , OH^- and $-OH$ groups on cellulose. As a result the observed $-OH$ diffusion coefficient is a population weighted average of the diffusion coefficients in the three sites⁵⁰.

If a binding process is reversible and occurs on a time-scale similar to that of the diffusion measurement, it is possible to learn additional information on the dynamics of the exchange process⁵. In figure below 2.4, a representation of a low molecular weight

species exchanging between being free in solution and being located in one for the binding sites of cellulose (a high weight species) is represented. K_d is the dissociation constant and represents the ratio of dissociated ions (products) to original reactants.

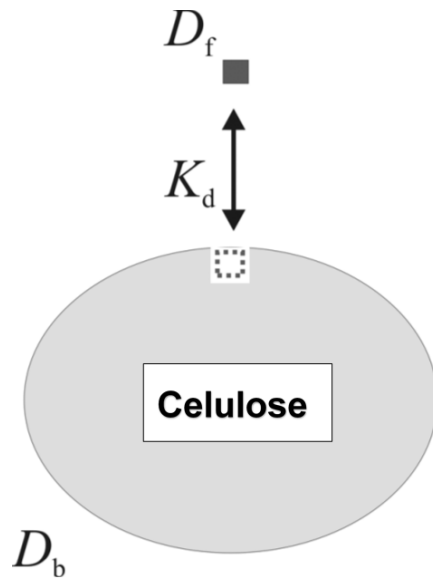


Figure 2.4. A schematic diagram of a two-site binding model of a ligand (square) with a free diffusion coefficient of D_f (D_{free}), in exchange with a binding site on cellulose. The diffusion coefficient of the bound ligand is D_b , and is taken as being equal to that of the cellulose. Adapted from Price⁵.

For a reversible and temporary binding, with residence time much shorter than the experimental observation time, i.e. in the fast exchange regime, the observed diffusion coefficient is a population weighted average. With two sites, that we denote “bound” (to cellulose) and “free” (in bulk), the following relation holds:

$$D = P_b D_b + (1 - P_b) D_{free} \quad (2.10)$$

P_b is the fraction bound, D_{free} is the diffusion coefficient of the unbound molecules and D_b is the diffusion coefficient of the bound molecules. During Δ , the solvent exchanges rapidly between the different sites, therefore we only “see” an average diffusion value¹¹².

Considering that the cellulose diffusion is equal to the value of the D_b , its assumed that value as zero (eq. 2.11) because cellulose diffuses considerably slower than the solvent (approximately two orders of magnitude). After some algebraic manipulation, the following relations can be established

$$D_b = D_{cell} = 0 \quad (2.11)$$

$$D = P_b D_{cell} + (1 - P_b) D_{free} \quad (2.12)$$

$$(1 - P_b) D_{free} \gg P_b D_{cell} \quad (2.13)$$

$$D_{free} = D_0 A \quad (2.14)$$

The obstruction factor A varies with concentration and D_0 is the diffusion coefficient of TBA+, water and DMSO in the pure solvent.

Assuming that:

$$\frac{D}{D_0} = A(1 - P_b) \quad (2.15)$$

D/D_0 represents the normalization of the solvent, where the measured diffusion coefficients for each concentration of cellulose are normalized by the diffusion coefficient of the solvent without cellulose.

The fraction of bound TBA⁺ is equivalent to the number of bound cations divided by the total, which is the sum of bound and free cations in solution and can be represented by eq. 2.16

$$P_b = \left(1 - \frac{D}{D_0}\right) \quad (2.16)$$

It is known that extremely weak acids, such as DMSO, are very unlikely to give away H⁺. Consequently, they have very low K_a (acid dissociation constant). To deprotonate such acids, very strong bases are required. If the pH in the solution is sufficiently higher than their pK_a, these compounds species may deprotonate¹¹³.

The solvent does not interact with an entire polymer chain at once. Therefore, it is necessary to scale the diffusion coefficient with respect to part of the chain. In this work we have considered the individual monomer unit –anhydrous glucose unit (AGU)¹¹⁴.

The TBA⁺ ions act as counterions to the deprotonated –OH groups on cellulose and thus are expected to interact electrostatically⁵⁰. Each monomer unit has 3 OH groups, all with a different pK_a. Through self-diffusion NMR, it is possible to estimate the average number α of TBA⁺ ions that are reversibly bound to each glucose unit via the following relation^{50,80}:

$$P_b = \frac{n_b}{n_{free} + n_b} = \frac{n_b}{n_{total}} = \frac{\alpha n_{AGU}}{n_{total}} = \alpha \frac{\frac{W_{AGU}}{Mw_{AGU}}}{\frac{W_{TBAH}}{Mw_{TBAH}}} = \alpha \frac{W_{AGU}}{1 - W_{AGU}} \times \left(\frac{Mw_{TBAH}}{Mw_{AGU}} \frac{1}{\beta} \right) \quad (2.17)$$

Where n_b is the number of bound molecules, n_{free} is the number of free molecules and n_{AGU} is the number of AGU units. Mw_{AGU} and Mw_{DMSO} are the molecular weights of AGU unit and DMSO and m_{AGU} and m_{DMSO} are the cellulose and DMSO weighted masses,

respectively¹¹⁵. The mass of weighted cellulose is divided by the total volume of the solution (2g), in order to obtain the mass fraction (W_{cell}).

Alpha, α , is the average number of ions – TBA⁺ in this work, that bind to each AGU unit. Previously, in order to obtain α , several calculations would be necessary in a time-consuming process, but with the faster method to obtain α , it is only needed to know the molecular weights, the weight fraction of cellulose and the normalized diffusion coefficients. The fraction of bound molecules, can be estimated by:

$$P_b = \left(\frac{\alpha}{\beta} \times \frac{MW_{TBAH}}{MW_{AGU}} \left(\frac{W_{AGU}}{1 - W_{AGU}} \right) \right) \quad (2.18)$$

Resulting in,

$$W_{TBAH} = (1 - W_{cell})\beta \quad (2.19)$$

Where β is the weight fraction of the solvent and $(1 - W_{cell}) = W_{solvent}$.

Replacing equation (2.18), in (2.15) we obtain,

$$\frac{D}{D_0} = 1 - \left(\frac{\alpha}{\beta} \times \frac{MW_{TBAH}}{MW_{AGU}} \left(\frac{W_{AGU}}{1 - W_{AGU}} \right) \right) \quad (2.20)$$

Rearranging the previous equation, α is obtained as follows

$$\alpha = \left(1 - \frac{D}{D_0}\right) \left(\frac{1 - W_{AGU}}{W_{AGU}}\right) \left(\frac{Mw_{AGU}}{Mw_{TBAH}}\right) \beta \quad (2.21)$$

2.5.2. The experiment

Different concentrations of cellulose were added to previously weighted TBAH (aq.) and mixed solutions of TBAH and DMSO in different ratios. Cellulose concentrations, ranging from 0.1 wt. % up to 6 wt. %, were dissolved in 30 wt. % and 55 wt. % TBAH (aq.). On the other hand, the 40 wt. % TBAH (aq.) was also mixed with DMSO in different ratios (1:1, 1:2, 1:3 and 1:4). Note that the 30 wt. % TBAH (aq.) solutions were obtained by dissolving cellulose in 40 wt% TBAH (aq.) and then diluting it with Milli-Q water. The formed solutions were stirred at maximum speed in an ARE stirrer made by VELP Scientifica. Samples were kept stirring at room temperature until fully dissolved. Their dissolution state was checked by polarized light microscopy. When dissolved, the samples were transferred into a NMR capillary and loaded in a 200MHz nuclear magnetic resonance spectrometer, Bruker Avance DMX200 spectrometer.

3. Results and discussion

3.1. Gelation of cellulose solutions dissolved in NaOH (aq.)

3.1.1. Rheometry and turbidimetry

The results of the time-resolved dynamic experiments of the 4 wt.% cellulose dissolved in 8% NaOH samples, show the influence of the temperature on the gelation time from 25 °C to 30 °C. Figure 3.1 are typical examples of such tests at different temperatures.

The gelation time t_{gel} was estimated from the crossover between G' and G'' (when $G' = G''$).

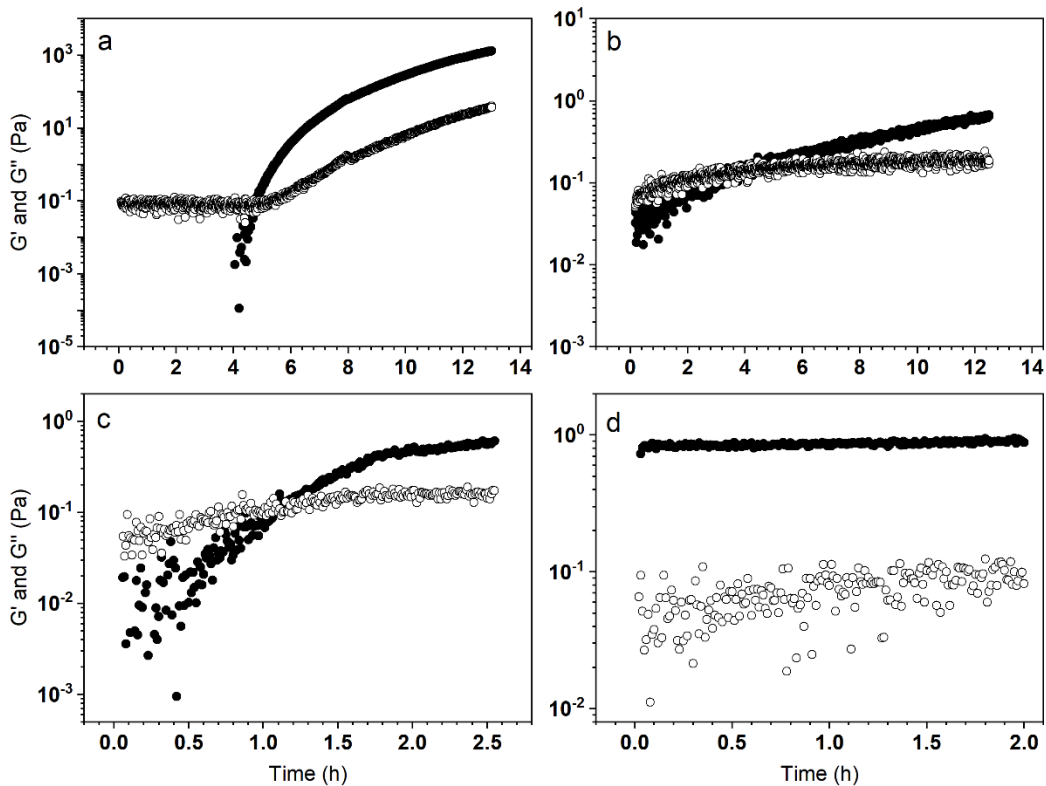


Figure 3.1. Loss, G'' , (empty circles) and storage, G' , (full circles) moduli time dependence at 25.0 °C (a), 27,5 °C (b), 29.5 °C (c) and 30 °C (d).

In figure 3.1, at 25 °C, G' was initially lower than G'' and thus the sample behaves as a viscous fluid. The crossover of G' and G'' was observed to occur at 16400s (4h and 34 minutes), indicating the gelation point. The dramatic increase in G' after crossover can be attributed to the initial fast rate of the network formation¹¹⁶. At a higher temperature at 27.5 °C, G' and G'' crossover is faster occurring after 12000 seconds (3h and 20 minutes). The same is observed with further increase of temperature to 29.5 °C where gelation is observed after 4000 seconds (1h and 7 minutes).

Once the temperature was set to 30 °C, the sample immediately gelled before any measurement. G' is always higher than G'' and frequency independent which is a typical rheological fingerprint of a gelled material.

The gelation points (estimated from the $G'=G''$) were compiled as a function of temperature (Figure 3.2).

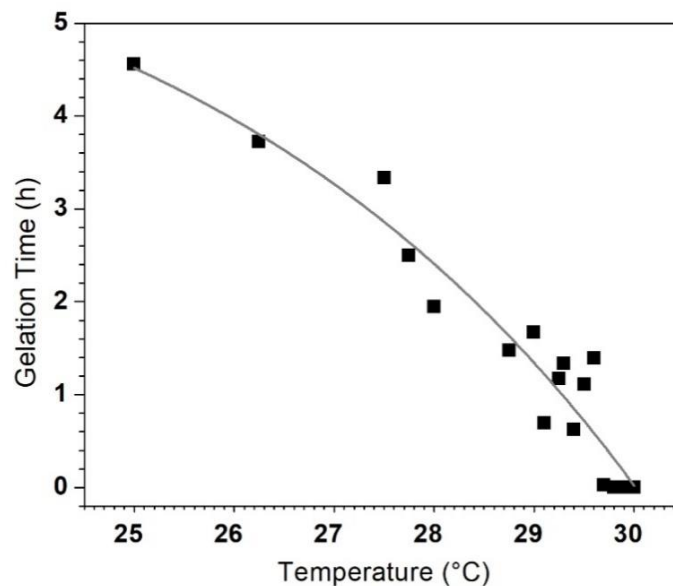


Figure 3.2. 4wt% cellulose in NaOH (2M) gelation time dependence with temperature. The line is just a guide for the eye.

As it is possible to observe in figures 3.1 and 3.2, the gelation process is strongly temperature dependent. It is striking that t_{gel} changes from several hours at room temperature to a couple of minutes/seconds for temperatures around 30 °C or above. The data in Figure 3.2 is consistent with the earlier work of Roy et al., who studied 5 wt% cellulose in 2.2 M NaOH (aq.)⁷⁰.

Recent SAXS measurements revealed that cellulose aggregation increases with increasing temperature, as shown by an increased scattering intensity at lower q values⁷¹. Variations in light scattering can also be followed by turbidity experiments⁷. In Figure 3.3.a, a time resolved turbidity study is reported where the temperature was alternating between 25 and 45 °C, being changed every 2 h.

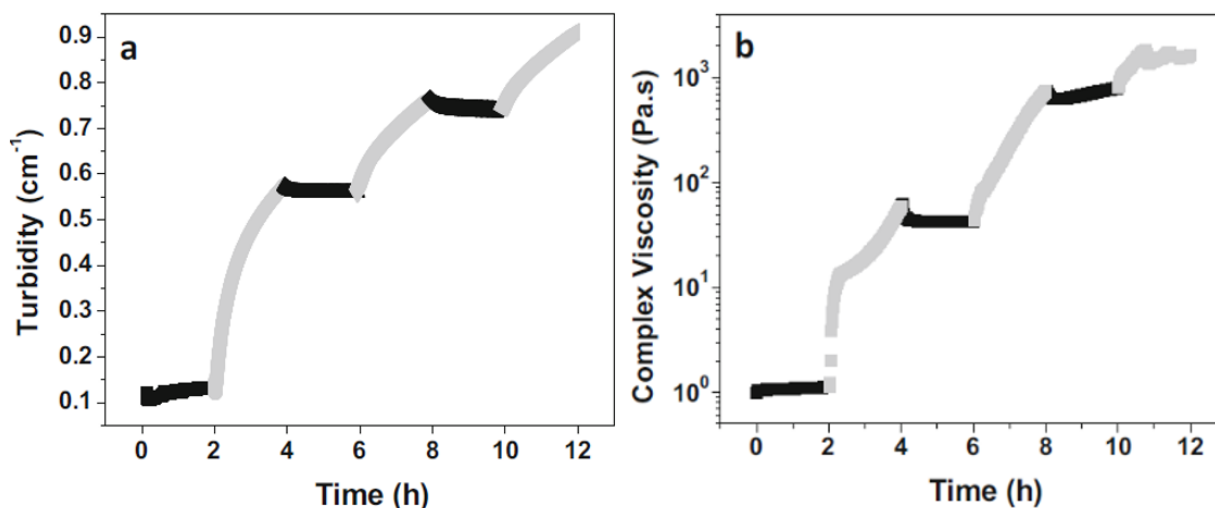


Figure 3.3. Turbidity (a) and complex viscosity (b) temperature experiments alternating between 25 (black symbols) and 45 °C (grey symbols) for 4 wt% cellulose in NaOH(aq.). Samples were kept for 2 h at each temperature before changing to the other temperature⁷.

As it can be observed in figure 3.3, the turbidity remains essentially constant when the temperature is 25 °C, while increasing with time at 45 °C. Showing that at 45 °C there is a gradual increase in cellulose aggregation, but no such increase is observed at 25 °C on

the time scale of 2 h. The fact that the turbidity and the complex viscosity are retained when lowering the temperature from 45 to 25 °C indicates that the aggregation is irreversible and that at 25 °C the solutions are only kinetically stable⁷. In Figure 3.3.b, the time evolution of the complex viscosity, following the same temperature cycling as in the turbidity experiments, is presented. As it can be seen, the viscosity data essentially follows the turbidity data⁷⁵. At 45 °C the viscosity gradually increases with time while it essentially remains constant when the temperature is 25 °C. The data in Figures. 3.3.a and 3.3.b clearly demonstrates (1) the coupling between the sample viscosity and the aggregation state of cellulose, (2) the irreversibility of the aggregation process, and (3) the significant difference in aggregation kinetics between 25 and 45 °C.

The irreversibility of the gelation process is also illustrated in Figure 3.4. The temperature was first increased from 10 to 40 °C and then decreased back to 10 °C at a constant heating rate of 0.1 °C/min and angular frequency of 1 rad/s in both directions. The evolution of G' and G'' are continuously monitored during a temperature ramp.

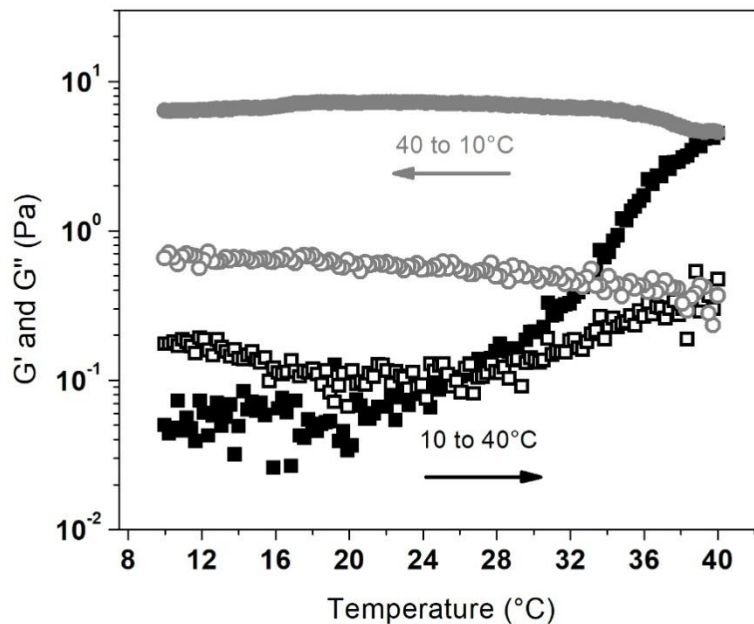


Figure 3.4. Temperature ramp test in the linear viscoelastic regime at frequency 1 1/s, the temperature was increased with 0.1 °C/min rate from 10 to 40°C (black) and then from 40 to 10°C (grey).

During heating from 10 to 25 °C, the sample behaves as a liquid-like solution with $G'' > G'$. At about 26 °C, G' and G'' crossover and G' increases strongly with increasing temperature. When the temperature is reversed from 40 to 10 °C, only minor changes are observed in respect to the final stage at 40 °C achieved with the first ramp test.

The most relevant information from figure 3.4 is that the transition is irreversible (as discussed in figure 3.3) when temperature is reversed from 40 to 10 °C, only minor changes are observed in respect to the final stage at 40 °C achieved with the first ramp test and no crossover was detected, prevailing the elastic behavior, with G' much higher than G'' ^{7,72}.

3.1.2. Wide angle X-ray Scattering

In order to shed light on the gelation mechanism and further characterize the aggregation of cellulose at elevated temperatures, WAXS was performed. All samples were loaded onto specific quartz capillaries and placed in the WAXS equipment.

A sample was stored at 45 °C and WAXS experiments were performed directly after preparation, and after 9 and 144 h. The solvent was subtracted to the measurement of our system. In figure 3.5 it is possible to observe different WAXS spectra recorded at different times.

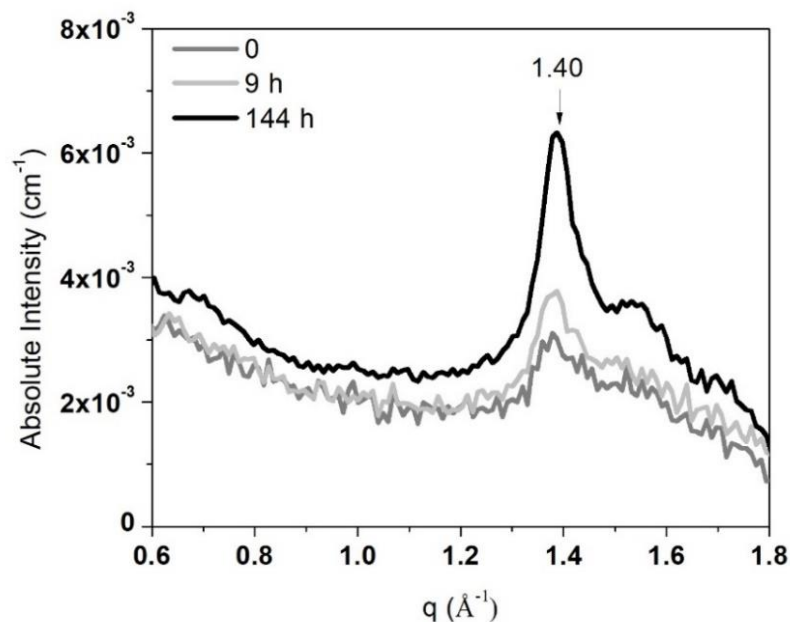


Figure 3.5. Solvent subtracted WAXS-patterns of freshly prepared (dark grey line), aged for 9 h (dark grey line) and aged 144 h (black line) 4 wt% of cellulose in NaOH (aq.) solutions at 45 °C. The arrow highlights the evolution of the main diffraction peak at $q = 1.4 \text{ \AA}^{-1}$.

A weak diffraction peak at $q = 1.4 \text{ \AA}^{-1}$ that grows in intensity with time can be observed. On the 144h sample, a second peak at $q = 1.55 \text{ \AA}^{-1}$ is also observed. The observed diffraction is attributed to the precipitation of crystalline cellulose, presumably partly as sodium salt due to the high pH⁷. The fact that only one or two diffraction peaks are observed suggests that crystallites are still small. The peak is not very broad, which indicates that there isn't a lot of amorphous material⁷⁶. The two reflections can be indexed to the 110 and 020 reflections of Na Cellulose IV crystals or Cellulose II¹¹⁷. The results are consistent with those of Isobe et al. who studied cellulose precipitation from alkali-urea solutions⁷⁴.

Gelation results from the self-aggregation of the cellulose chains in the solution with time (or temperature), due to crystallization and precipitation of cellulose^{7,51}. The aggregation is proposed to occur due to a minimal precipitation of cellulose II, where there will be crystalline domains (from cellulose II) surrounded by an entangled network of cellulose

^{172,80}.Precipitation of cellulose II has been recently suggested to occur in another strong alkaline system, 40 wt. % TBAH (aq.)⁸⁰. Cellulose II is a more stable crystalline form compared to native Cellulose I and therefore dissolving Cellulose I may result in a supersaturated state with respect to Cellulose II that (slowly) precipitates. Thus, it is here suggested that the observed gelation is due to the precipitation and crystallization of cellulose. A cartoon on the hypothetical gel structure is shown in Figure 3.6 where cellulose chains may participate in more than one crystallite to form the 3D cross linked network.

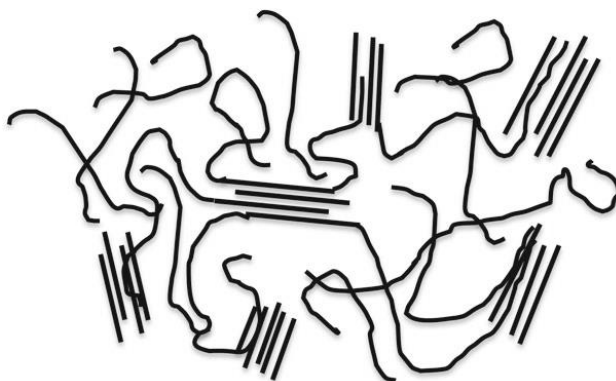


Figure 3.6. Illustration of the gel structure obtained from cellulose crosslinking where the crystallites are suggested to work as junction points⁷.

Polymer crystallization is a complex process, possibly involving multiple kinetically trapped states¹¹⁸. In the nucleation and growth process, the long chain molecules may be part in more than one crystallite. The crystallites may thus compete for the same molecule and, moreover, such crystallites can act as effective cross-linkers. Gelation is, in fact, a general feature of polymer crystallization and this has been extensively studied for e.g. poly(vinyl alcohol), PVA¹¹⁹⁻¹²².

3.2. Solvent interaction with cellulose: role of water, cosolvent and TBA⁺ cation

3.2.1. Self-diffusion NMR

Previous data suggests that replacing sodium with the more hydrophobic tetrabutyl ammonium cation, TBA⁺, improves cellulose solubility⁵⁹. While Na⁺ as a small cation, fits well into the dense crystalline lattice of cellulose, resulting in a stable crystalline phase, the same cannot be achieved when replacing it with a more bulky organic cation, such as TBA⁺, as it is too big to fit in the crystalline lattice, then the salt crystal becomes unstable and large amounts of cellulose can be solubilized as seen by Gubitosi et al.^{18,76}. Furthermore, due to its inherent amphiphilicity, TBA⁺ can interact with the respective hydrophobic regions in cellulose enhancing its dissolution, which is not observed for the small inorganic Na⁺ in the NaOH (aq) system^{43,47}.

The addition of DMSO to the TBAH (aq.) system is expected to improve the dissolution, as observed by Medronho et al.¹²³; however, the role of the DMSO is not yet fully understood^{85,124}.

With this background in mind, different concentrations of cellulose, ranging from 0.1 wt.% up to 6 wt. %, were dissolved in 30 wt. % and 55 wt. % TBAH (aq.). In addition, cellulose was also dissolved in mixed 40 wt. % TBAH (aq.) with DMSO in different ratios (1:1, 1:2, 1:3 and 1:4), as described in the experimental section.

It was observed that cellulose is more easily solubilized in 55 wt. % TBAH (aq.) than in lower concentrations of the solvent. On its own, the 30 wt. % TBAH (aq.) and lower concentrations do not dissolve cellulose efficiently but, surprisingly, the addition of DMSO promotes cellulose dissolution with a TBAH content as low as 7 wt. %.

Self-diffusion NMR, as mentioned above, can be used to determine the diffusion of molecules and aggregates, as well as the degree of polymerization or size of a solvation

shell⁵⁰. In this work, we use this method to investigate the solvent-solute interactions and determinate the effect of DMSO as a co-solvent in the dissolution of cellulose.

The experimental parameters used in this work were the same as Gentile et al.⁸¹ Therefore, to access the H₂O–OH, DMSO and TBA+ self-diffusion coefficients the parameters used were as follows: D = 140 ms, d = 2 ms and g was varied from 0 to 16 g/cm for H₂O–OH and from 25.3 to 101.1 g/cm for TBA+ in 16 gradient steps. Figure 3.7 reports the experiments performed on one sample taken as example, where the decay of the signal can be observed with gradient strenght.

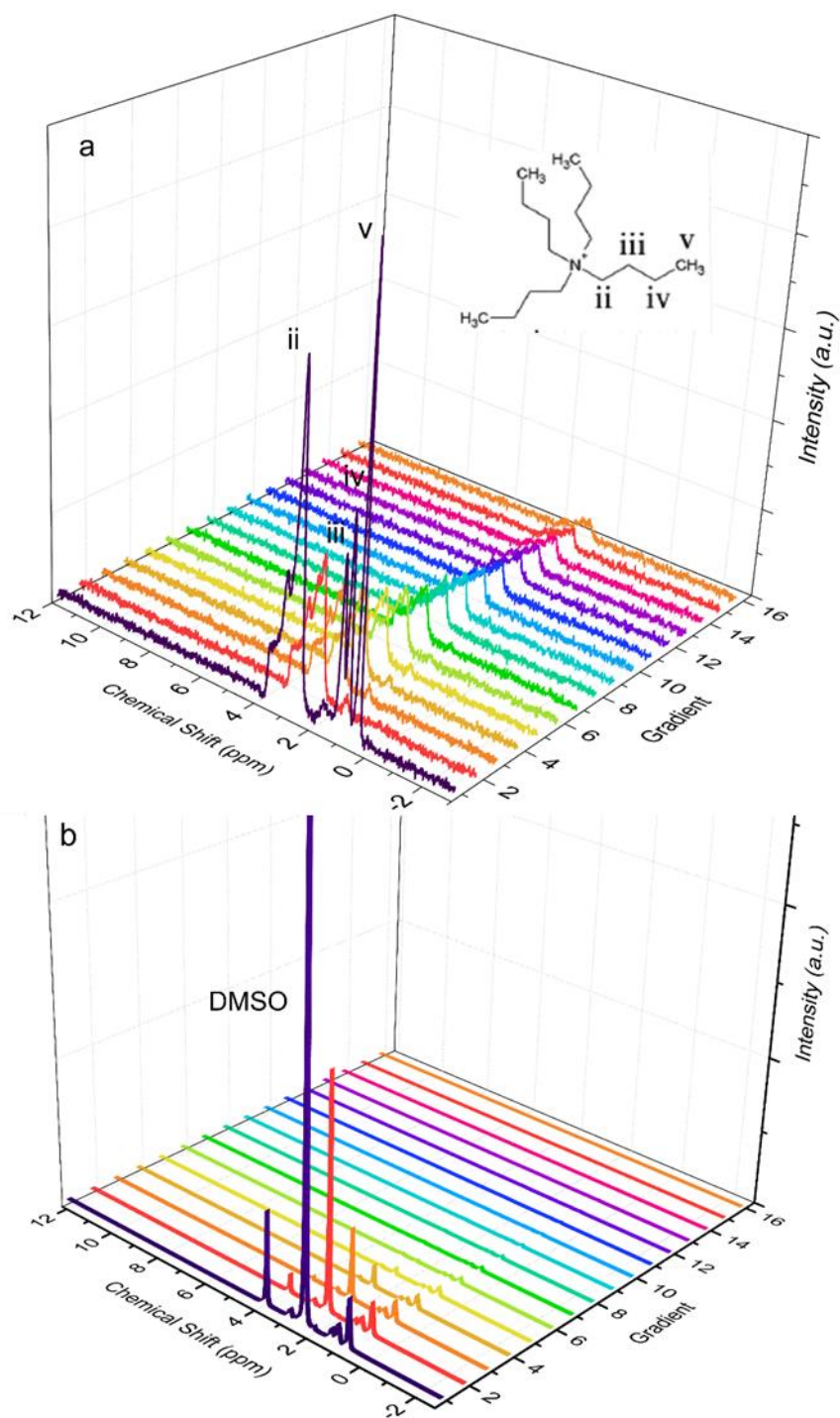


Figure 3.7. Schematic illustration of the self-diffusion experiments. The sample consists of 4 wt% of cellulose in 40 wt% TBAH/DMSO mixture (1:4 ratio) at 25 °C. The experimental parameters to measure H₂O–OH, DMSO (b) and TBA⁺ (a) self-diffusion coefficients were $D = 140$ ms, $d = 2$ ms and g was varied from 0 to 16 g/cm for H₂O–OH and from 25.3 to 101.1 g/cm for TBA⁺ in 16 gradient step.

Data was treated as described in chapter 2.5.1.

3.2.1.1. Relative Diffusion Coefficient

According to Price⁴, the diffusion coefficient of a species in solution is directly related to its hydrodynamic properties, which are in turn related to the size and shape of the species, the solvent viscosity and other intermolecular interactions, such as exchange and obstruction.

In figure 3.8, the relative diffusion coefficients of TBA⁺, DMSO and water as a function of cellulose weight fraction in a TBAH/DMSO mixture (1:4 ratio) at 25 °C and 30 °C, are compared.

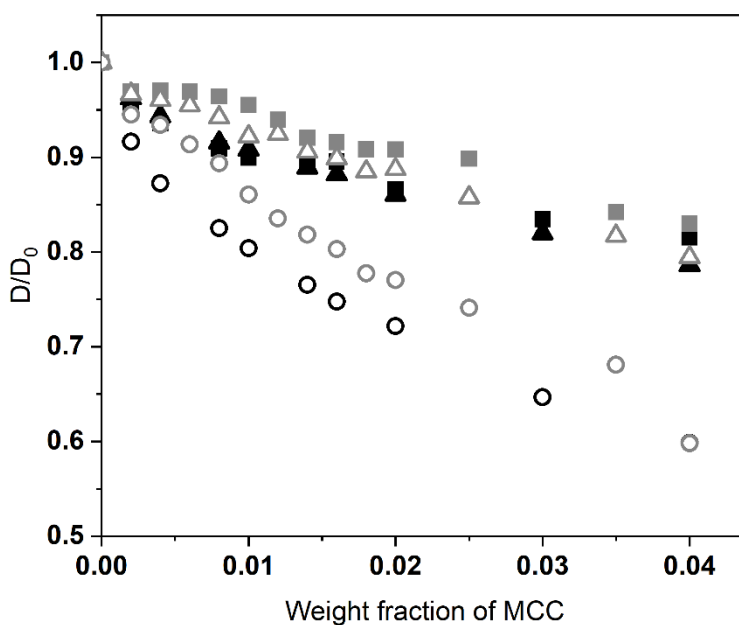


Figure 3.8. Relative diffusion coefficients of TBA⁺ (circles), DMSO (triangle) and water (squares) as a function of cellulose concentration in a TBAH/DMSO mixture (1:4 ratio) at 25 °C (grey) and 30 °C (black). Note that a 40 wt. % TBAH (aq.) was used here.

Higher diffusion coefficients mean that molecules will diffuse faster in the medium they are in, into each other. It is observed that the TBA⁺ diffusion coefficients decrease essentially linearly with the cellulose concentration. The addition of colloidal particles (in this case, cellulose chains) are expected to reduce the solvent diffusion coefficient because of obstruction of diffusion paths (an excluded volume effect)^{81,111}. Nevertheless, and as observed by Gentile and Olsson⁸¹, the diffusion coefficient of TBA⁺ has a much stronger concentration dependence than what could be explained by “simple” obstruction effects. Assuming that cellulose can be regarded as cylinder-like molecule, the obstruction corresponds only to a reduction of the diffusion coefficient by a few percent at the highest cellulose concentration used here (i.e., 4 wt.%). Again, the obstruction effects alone cannot explain the dependence of the solvent diffusion coefficients with the cellulose concentration.

The decrease of the TBA⁺ self-diffusion coefficient with the cellulose concentration is consistent with a saturated fixed number of bound TBA⁺ ions per cellulose molecule, but with fast exchange with the bulk, on the experimental time scale, so that only an average TBA⁺ diffusion coefficient is observed⁸¹. In this case, the observed diffusion coefficient is a population weighted average^{81,125}.

The same type of analysis could be done on the water/OH⁻ diffusion and DMSO. Even though the water, on a molar basis, is in considerable large excess, the effect of possible binding on the water diffusion is expected to be small, but still quantifiable.

The TBA⁺ self-diffusion behaviour, as a function of cellulose concentration, is due to the interactions with their environment, i.e., cellulose, independently from the cellulose molecular weight, since the same cation/ glucose unit ratio in MCC and pulp was reported by Gentile and Olsson⁵⁰. These interactions are slowing down the motion of the TBA⁺ relative to the water. On the other hand, the effect of DMSO on these self-diffusion behaviours translates into a higher diffusion coefficient obtained at lower concentrations of TBAH, in relation to the results obtained by the relative coefficient diffusion obtained by Gentile and Olsson for samples without DMSO⁸¹. The water and DMSO self-diffusion is

not very affected by cellulose concentration. The minor decrease in self diffusion is, most likely, due to the increasing viscosity of the system with cellulose concentration.

Another observation from Figure 3.8, is that temperature has a slight effect on the diffusion coefficient values. Surprisingly, the diffusion values at 30 °C are lower than the ones measured at 25°C, but the difference is not significant. The increase in temperature would be expected to raise the diffusion coefficients as typically observed when the kinetic energy is increased. Perhaps the higher temperature favours a more molecular focused dissolution, where cellulose chains will be better dissolved at 30 °C than at 25 °C. If more cellulose molecules are available at high temperature (improved dissolution) there is a higher probability to interact with TBA⁺ decreasing the average diffusion coefficient observed. Partial cellulose aggregation induced by the higher temperature may also contribute to this effect.

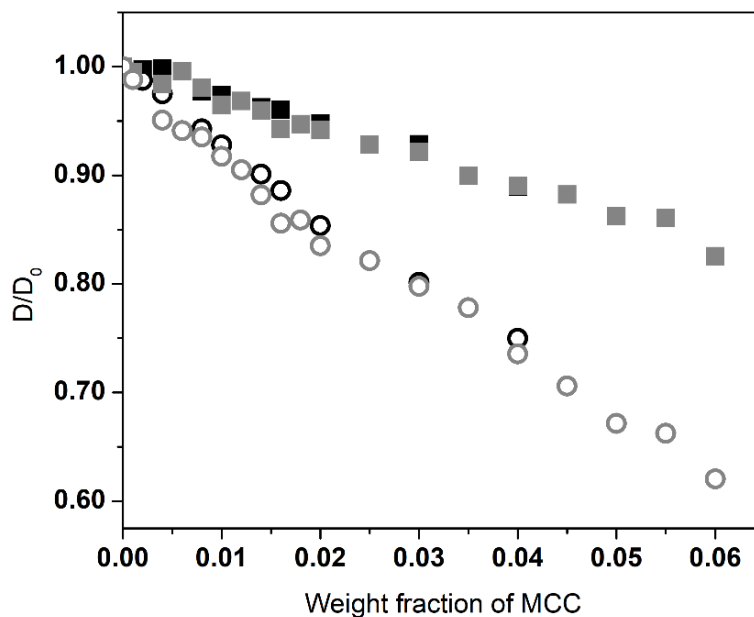


Figure 3.9. Relative diffusion coefficients of TBA⁺ (circles) and water (squares) as a function of cellulose concentration in a 55 wt% TBAH (aq.) solvent 25°C (grey) and 30°C (black). Note that the solvent used was a 55 wt% TBAH in water.

The same pattern regarding the temperature effect seen in figure 3.8 was not observed in figure 3.9 where DMSO is not present. Here, no significant differences in the diffusion coefficients are observed for both temperatures. This may suggest that the presence of DMSO can affect the diffusion behaviour of water and TBA+ cation. Perhaps, at high temperatures, DMSO is more available to establish hydrogen bonds (via its sulfoxide group) with water and TBA+ slowing down their diffusion. Nevertheless, the DMSO role is not yet fully understood.

In figure 3.10, a comparison of the relative diffusion coefficients of TBA+, DMSO and water is represented as a function of cellulose weight fraction in the solvent system composed of 40wt% TBAH (aq.) and DMSO at different ratios (1:1; 1:2; 1:3 and 1:4).

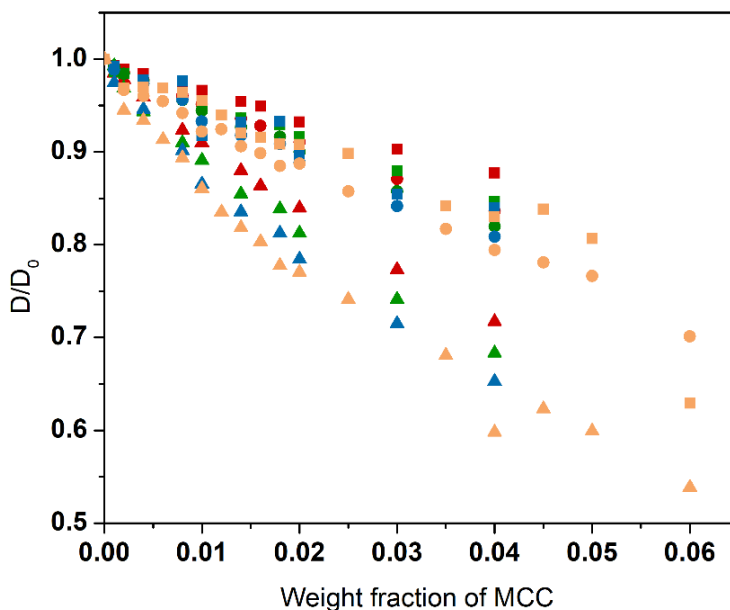


Figure 3.10. Comparison of the relative diffusion coefficients of TBA+ (circles), DMSO (triangles) and water (squares) as a function of cellulose weight fraction in the solvent system composed by 40wt% TBAH (aq.) and DMSO at 1:1 (red); 1:2 (green); 1:3 (blue) and 1:4 (orange) TBAH/DMSO ratios.

Previously, the addition of DMSO was observed by Medronho et al¹²⁰. to be beneficial for cellulose dissolution, because lower TBAH concentrations could be used without significantly compromising the dissolution performance. This is important because DMSO decreases the overall viscosity of the dope (being easier to manipulate it) and the solvent system becomes less expensive with a low content of active compounds, TBAH.

From Figure 3.10, it is possible to observe that the TBAH/DMSO ratio influences the diffusion coefficients. For the same cellulose concentration, the higher the DMSO content the lower the diffusion coefficients of all species (i.e., water, DMSO and TBA⁺). This observation might be related to the beneficial effect of DMSO in cellulose dissolution. It is suggested that the presence of DMSO enhances cellulose swelling and dissolution more efficiently and therefore more cellulose individual molecules disaggregate from microfibrils and are available in solution. As consequence, the number density of cellulose molecules per unit volume increases as the interactions between cellulose and all the other species in solution. A linear decrease in the diffusion is also observed for all the TBAH-DMSO ratios when the cellulose concentration is increased. This observation is in agreement with previous NMR self-diffusion studies⁵⁰. According to these studies, the addition of particles to the solution hinders the diffusion of the solvent due to obstruction paths^{50,111}. The differences in the diffusion coefficient are not significant for the water and DMSO in the different TBAH/DMSO ratios. On the other hand, the differences of the diffusion values are superior for the TBA⁺ case since its concentration is decreasing with the addition of more DMSO and therefore a lower concentration of cations is present in the bulk.

3.2.1.2. Percentage of bound molecules and alpha values

Following the data analysis described in 2.5.1, the α values and P_b were calculated. Note that α can be regarded as the average number of ions – TBA⁺ in this case, that “bind” to

each AGU unit, while Pb represents the number of “bound” molecules of DMSO, TBAH or H₂O to cellulose, out of the total amount in solution (i.e., free + bound).

In the next figures, Pb and α values are compared as a function of cellulose weight. Note that for the α determination the values obtained below a cellulose weight fraction of 0.005 were not considered due to high uncertainty error associated. In figure 3.11, a comparison of Pb and α values for 40 wt. % TBAH (aq.)/DMSO (1:4 ratio) and 55 wt. % TBAH (aq.) as a function of weight fraction of cellulose at 25 °C and 30 °C is represented.

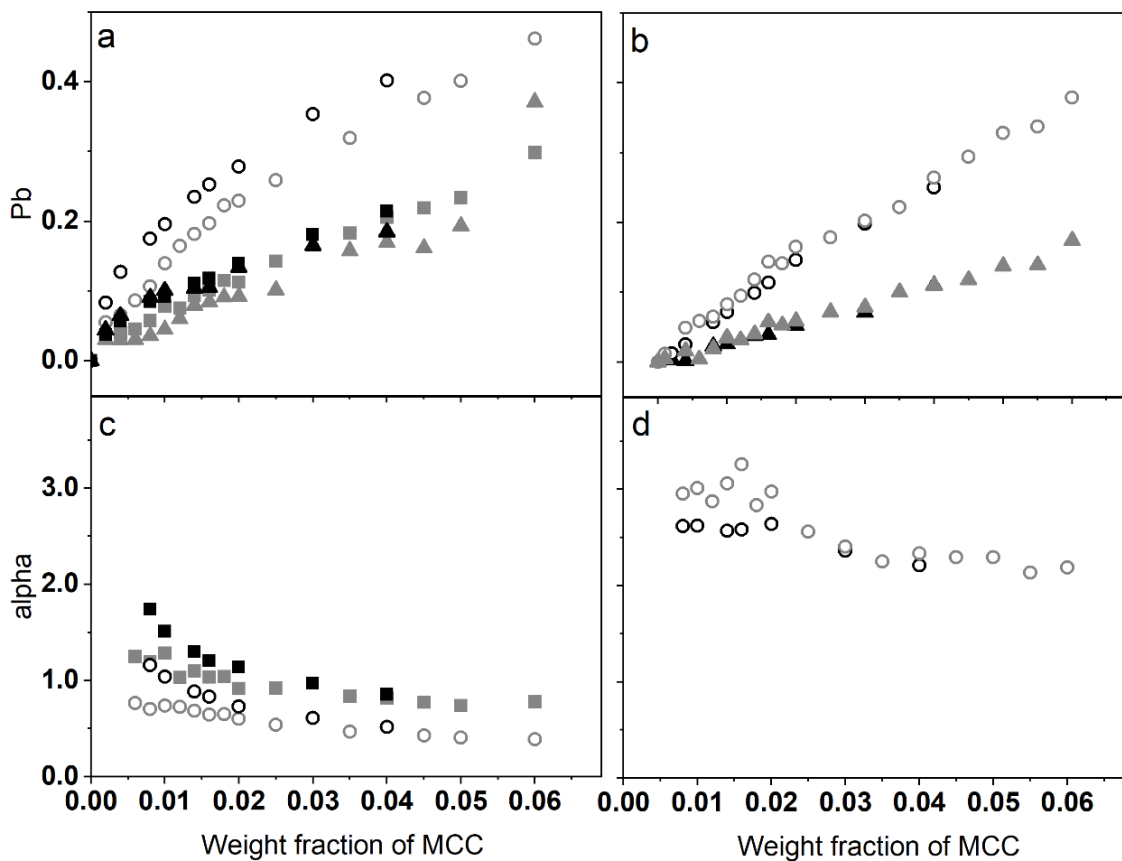


Figure 3.11. Fraction of Pb (a and b) and α values (c and d) of DMSO (squares), TBAH (circles) and water (triangles) as a function of cellulose weight fraction. The solvent system used is a 40 wt% TBAH (aq.)/DMSO (1:4 ratio) (a and c) and 55 wt% TBAH (aq.) (b and d) at 25 °C (gray) and 30 °C (black).

As it can be observed in figures 3.11.a and 3.11.b, the P_b increases with increasing cellulose concentration for TBA⁺, DMSO and water in solution for both systems, 40 wt. % TBAH (aq.) with DMSO and 55 wt. % TBAH (aq.) without DMSO. On the other hand, in figures 3.11.c and 3.11.d, the α values for TBA⁺ decrease with the increase of cellulose in solution. The α values are also observed to be higher in the system without DMSO. In the 40 wt. % TBAH (aq.) with DMSO, there is a smaller quantity of TBA⁺ cations in solution and even if the pH could be high enough to keep the cellulose charged the same way as in the 55 wt. % TBAH (aq.) system, the TBA⁺ ions will also be conditioned by the role of DMSO. As the diffusion results in figures 3.8 and 3.10 showed, DMSO has a diffusion coefficient close to water and thus must also be solvating cellulose. DMSO is known to be a good swelling agent but the mechanism and its interactions with cellulose are not fully clear.

Cellulose concentration effect: Mixtures with higher DMSO concentration have higher percentages of bound molecules, while mixtures with lower DMSO concentration, or without DMSO have lower fraction of bound molecules. The stoichiometric ratio is higher in the beginning since there is less cellulose and lower viscosity as opposed to higher concentrations of cellulose where viscosity is higher. As the number of entanglements increases with the increase in cellulose in solution, the binding of TBA⁺ to cellulose will be diffculted due to increase of effects, such as steric hindrance and viscosity.

Temperature effect: regarding the temperature, there is no apparent effect of it on the percentage of bound molecules of TBA⁺ and water for the 55 wt. % TBAH (aq.) system, as observed in figures 3.11.b and d. While in the solvent system with DMSO and 40 wt.% TBAH (aq.), there is a slight difference in the P_b and α values obtained at 25 and 30 °C.

The same behaviour was observed for all the other TBAH/DMSO ratios for the different temperatures studied (see figures in the appendix section).

On the following table, the Pb at 4 wt. % cellulose, in 55 wt. %TBAH (aq.), 30 wt. % TBAH (aq.) and mixtures with different ratios of 40 wt. %TBAH (aq.) with DMSO (i.e., 1:1, 1:2, 1:3 and 1:4 ratio) is summarized:

Table 3.1. Pb at 4 wt. % cellulose for different solvent systems studied.

T (°C)	Solvent system	TBA+ (%)	DMSO (%)	H ₂ O (%)
	TBAH (40) - DMSO (1:4)	40	21	17
25	TBAH (40) -DMSO (1:3)	35	19	16
	TBAH (40) -DMSO (1:2)	32	18	15
	TBAH (40) -DMSO (1:1)	28	16	12
	TBAH 30%	23	-	9
	TBAH 55%	26	-	11
30	TBAH (40) - DMSO (1:4)	40	21	18
	TBAH 55%	25	-	11

The results in table 3.1, show that the Pb of TBA+ is highest when the TBAH weight fraction is lower at 1:4 ratio, and decreases with the increase in TBAH in solution. The same pattern is observed for DMSO and H₂O. In regard to temperature, the same values of Pb were obtained for both temperatures in 55 wt. %TBAH (aq.) In figure 3.12, the Pb values from table 3.1 for 4 wt.% cellulose are represented for all the TBAH concentrations and different ratio mixtures with DMSO studied.

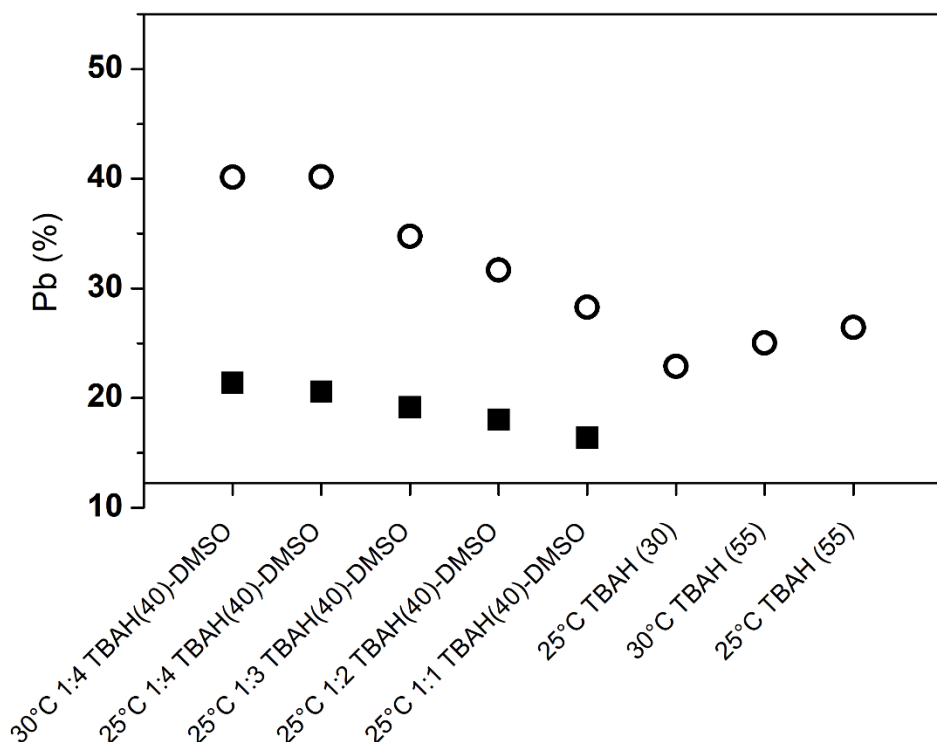


Figure 3.12. Summary of fraction of bound molecules of TBA⁺ and DMSO for 4 weight percent cellulose in solutions of different quantities of TBAH (30%, 40%, 45% and 55%) and different ratios of TBAH (40%) with DMSO at 25 °C and 30 °C.

Figure 3.12 and table 3.1, show that the fraction of TBA⁺ and DMSO molecules bound to cellulose decreases with higher TBAH concentrations. The highest Pb is 40% bound molecules for the lowest TBAH concentration and it gradually decreases as we increase the TBAH concentration. This pattern could be caused by stereochemical effects; Since TBA⁺ is a bulky cation, when in lower concentration, it will be easier to approach the cellulose molecules and interact with its deprotonated OH groups, as well as with the hydrophobic regions of cellulose. With the increase of TBAH and reduction of DMSO in solution, the steric effect is more pronounced and TBA cations will be hindered to interact with cellulose due to the competition (for space) with other TBA⁺ ions for cellulose. For higher DMSO concentrations, the hydrophobic effect seems to be enhanced (DMSO

enhances dissolution and exposes more efficiently the less polar areas of cellulose to the solvent) and therefore there will be more interactions between TBA⁺ and cellulose hydrophobic areas.

In table 3.2., the average α values obtained for the dissolution of cellulose in 55 wt. %TBAH (aq.) and 30 wt. %TBAH (aq.) and mixtures with different ratios of 40 wt. %TBAH (aq.) with DMSO (i.e., 1:1, 1:2, 1:3 and 1:4 ratio), are summarized.

Table 3.2. α values obtained through self-diffusion NMR data fittings.

Sample/ Temperature		1:4 TBAH(40) /DMSO	1:3 TBAH(40) /DMSO	1:2 TBAH(40) /DMSO	1:1 TBAH(40) /DMSO	TBAH (30)	TBAH (55)
α	25 °C	0.52	0.56	0.67	0.90	1.1	2.3
	30 °C	0.52	-	-	-	-	2.2

The α values increase (number of bound TBA cations to glucose units) with the increase in TBAH concentration in solution. At the lowest concentration of TBAH, in the 1:4 ratio mixture, only a mean of 0.52 TBA⁺ ions bind to each AGU unit; whereas at the highest concentration of 55 wt. %TBAH (aq.), there is an average of 2.3 TBA⁺ ions bound per AGU unit. The temperature does not appear to affect α .

On figure 3.13, we compare the TBA⁺/AGU ratios for different quantities of TBAH (30, 40 and 55 wt. %) and different ratios of DMSO with 40 wt. %TBAH (aq.) at different temperatures, 25°C and 30°C, represented in table 3.2.

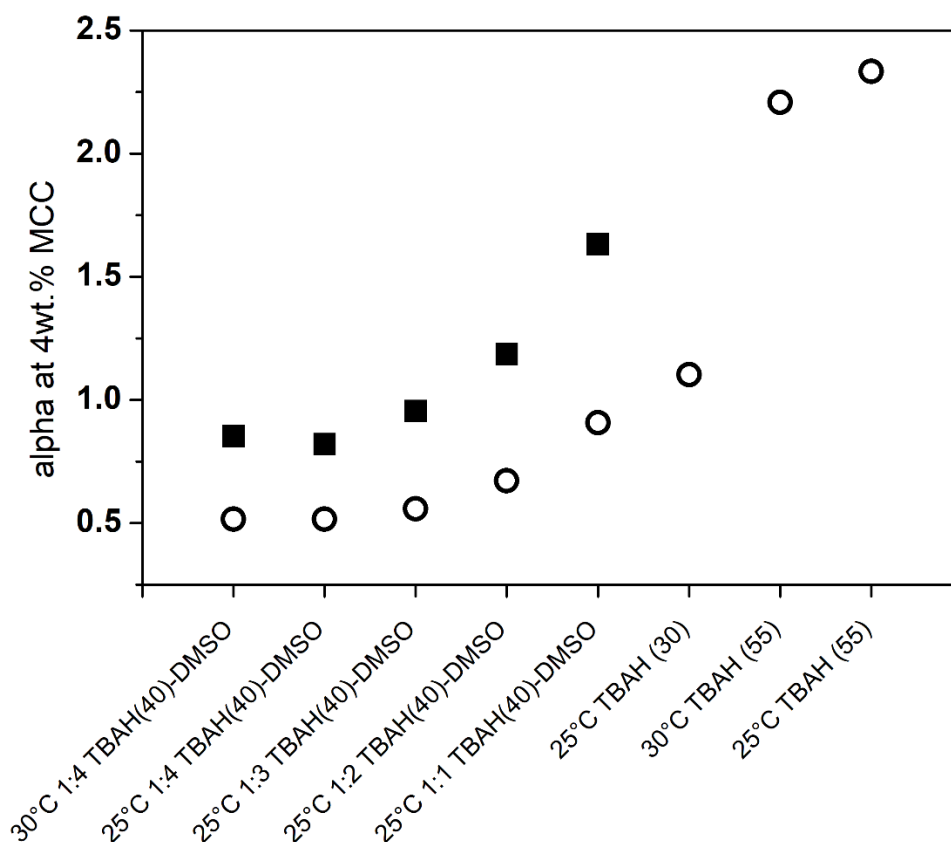


Figure 3.13. Summary of α values for 4 wt. % cellulose in TBAH solutions of different concentrations (30, 40, 45 and 55 wt. %) and different ratios of 40 wt. % TBAH (aq.) with DMSO at 25°C and 30°C.

The α values represented in table 3.2 and figure 3.7. seems to follow a trend as we increase the TBAH concentration in solution. With 7 wt. % TBAH in solution (for the highest DMSO used), α is approximately 0.5, and slowly increases until 2.3 when we have 55 wt. %TBAH (aq.). For higher TBAH concentrations, there could be an increase on pH, and for TBAH concentrations above 40 wt. % we obtain an average of bound TBA+/AGU above 2, which might indicate the titration of the second OH group. The electrostatic factor in the interaction of TBA+ with cellulose, which is partially ionized, will decrease. This suggests that the higher the cellulose ionization, the higher the number of TBA+ ions bound per AGU.

In figure 3.14, the α values are represented as a function of the weight fraction of TBAH present in the solvent.

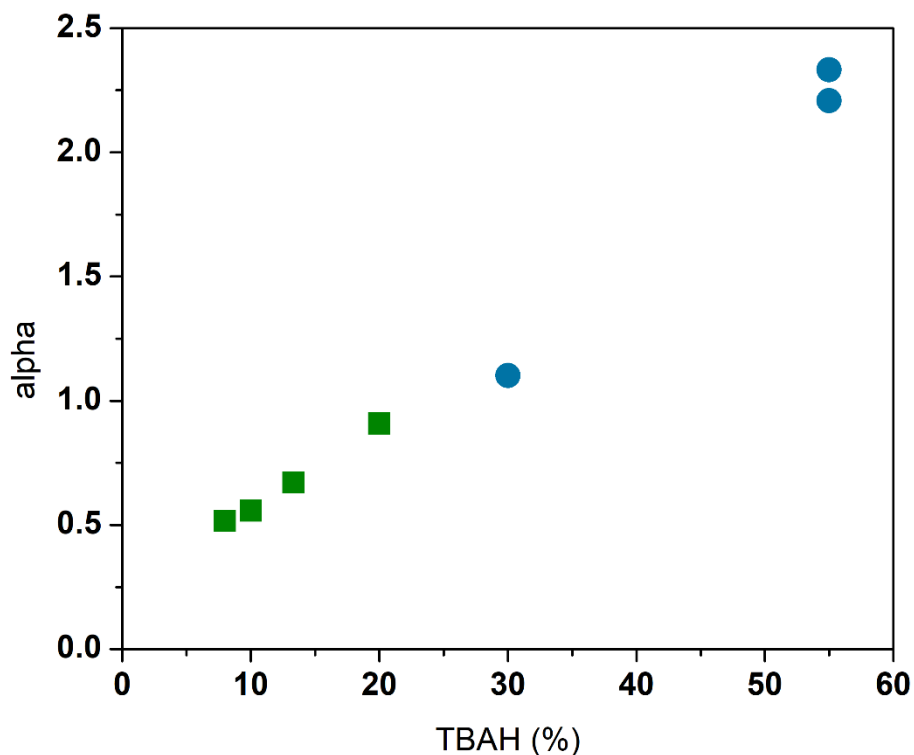


Figure 3.14. Summary of α values for 4 wt. % cellulose as a function of the weight fraction of TBAH present in the different solvents used. Green symbols represent the solvents containing DMSO, while the blue symbols represent the systems without DMSO.

Apparently, as the amount of TBAH in solution is increased, the TBA⁺ cations available to bind to cellulose also increase thus raising α . As mentioned before, the OH groups in each AGU unit of cellulose have different pK_a. Data suggests that below 40 wt.% TBAH it is only possible to ionize one OH group per AGU, while above 40wt.% it is possible to ionize ca. 1 OH groups per AGU. The number of TBAH molecules around cellulose is proportional to the weight fraction of TBAH and reaches a limit of ca. 2 TBA⁺ binding to the cellulose monomers (on average) for concentrations of TBAH above 50 wt. %. It is

very unlikely to reach 3 TBA⁺ binding to AGU, due to steric effects, as TBA⁺ is a quite bulky cation¹²⁶.

Overall, if solvent molecules reversibly associate or bind to cellulose, they will diffuse together with cellulose and present a lower diffusion coefficient. The binding can be electrostatic, as in the case of the TBA⁺ ion, or hydrogen bonding, in the case of DMSO and water. In addition, hydrophobic attraction between cellulose and TBA⁺ and DMSO might occur due to their structural features.

It was observed that cellulose is more easily solubilized in 55 wt. % TBAH (aq.) than in lower concentrations of the solvent. 30 wt. % TBAH (aq.) and lower concentrations, do not dissolve cellulose on its own, but dissolution occurs when adding DMSO, promoting cellulose dissolution with a TBAH content as low as 7 wt. %. If the cellulose is less charged, dissolution would be expected to be less favourable.

DMSO cannot dissolve cellulose by itself and its the role is not yet fully understood¹²⁴. Addition of low concentrations of DMSO is known to decrease the viscosity of ILs and enhancing the dissolution of cellulose by weakening the electrostatic ion-ion interactions and it is believed that DMSO modifies and widens the crystalline structure of cellulose, interacting with hydroxyl groups by possibly forming hydrogen bonds on cellulose, thereby stabilizing the cellulose chain and preventing it from further reforming inter- and intramolecular hydrogen bonds^{85,127–129}.

As observed by Wei et al.³⁸ in the TBAH/Urea solvent system, our TBAH/DMSO solvent system could have DMSO working as an hydrophobic contributor, by which the amphiphilic properties of the solvent could be adjusted. Having a similar amphiphilicity of natural cellulose's crystal surface, the interfacial resistance between cellulose and the solvent can be reduced, so that the crystal of cellulose can be better infiltrated and consequently dissolved by the solvent³⁸. In the results obtained by Huang et al.¹²⁸ for the TBAA/DMSO solvent system, both TBA⁺ and DMSO form a sheath around the cellulose

chain to prevent the combination of cellulose and support the dissolution of cellulose¹²⁸, as it was also observed by TBA⁺ in other experimental work for TBAH alone^{50,59,80,130}. If such mechanism occurs in parallel in our system, it is reasonable to assume that the TBA⁺/DMSO interaction can compete with TBA⁺/cellulose and DMSO/cellulose. Therefore, the α of DMSO is observed to increase as more TBA⁺ becomes available in solution (e.g., going from a TBAH/DMSO ratio of 1:4 to 1:1). This mechanism might be occurring in our TBAH/DMSO systems.

4. Conclusion

Cellulose gelation in 2 M NaOH(aq) has been studied by time resolved rheology and wide angle X-ray scattering. We find that the gelation kinetics is strongly temperature dependent, increasing rapidly with increasing temperature. Wide angle X-ray scattering data reveals the formation of crystalline domains, as the sample gels, and we conclude that the gelation is due to the crystallization and precipitation of cellulose. We also note that this kind of gelation is a common feature of polymer crystallization from solution.

The molecular self-diffusion coefficients were measured in cellulose solutions dissolved in 30 wt. %, 55 wt. % and mixtures of 40 wt. % TBAH (aq.) and DMSO at different ratios. The dissolution efficiency of TBAH (aq.) is not compromised significantly even when high amounts of the organic co-solvent (DMSO) are present in agreement with previous studies. Compared with the standard TBAH (aq.) solvent, 55 wt. % TBAH (aq.) the systems with DMSO presented in this work are highly advantageous since they use much less TBAH (substituted by DMSO) making the dissolution process much less expensive and possibly viable for large scale applications.

The molecular self-diffusion coefficients results highlight that TBAH can bind to cellulose within an interval of 0.5 TBA⁺ to 2.3 TBA⁺ per anhydroglucose unit depending on the TBAH amount in solution. The main driving force for this binding may be the favourable electrostatic attraction between the TBA⁺ cations and the deprotonated hydroxyl groups on the cellulose molecules coupled with hydrophobic interactions. The number of TBA⁺ ions around cellulose is proportional to the weight fraction of TBAH and reaches a limit of ca. 2 TBA⁺ binding to the cellulose monomers (on average). Since TBA⁺ is a quite bulky cation, it is very unlikely to reach 3 TBA⁺ binding to AGU, due to possible steric effects. Moreover, the number of cations involved in the solvation process seems to be fairly independent from temperature, at least in the temperature range studied which was quite small. We do not rule out the possibility of a higher thermal effect for higher temperatures. Temperature seems to not have a significant effect on the relative diffusion coefficient of the different species either in the presence or absence of DMSO in the mixture.

5. Future work

We believe this study has contributed with interesting findings regarding the improvement of our understanding of the dissolution and gelation phenomena of cellulose dissolved in cold alkali.

To further explore this topic, other co-solvents and/or additives could be investigated to shed light on cellulose's dissolution and gelation processes. Additionally, the concentration of NaOH could be extended to lower and higher values within the dissolution window.

Understanding the way cellulose is organized, how it interacts with other molecules and which structures are formed is very important in order to develop new and improved materials, as well as to provide important hints regarding the dissolution mechanism.

Therefore, regarding the TBAH-based systems, additional studies could be done to better understand the way TBAH and cosolvents interact with cellulose.

- Which is the effect of DMSO's addition, its role in the dissolution and the way it interacts with cellulose. This is still an open question needing systematic work to clarify it.
- The temperature range and concentrations of TBAH, DMSO and cellulose could be varied and explored.
- Exploration of new co-solvents or additives as suggested for the NaOH. Candidates include urea, thiurea, surfactants, and other molecules known to weaken hydrophobic interactions and eventually tune the dissolution process.

References

1. Postek, M. T. *et al.* Development of the metrology and imaging of cellulose nanocrystals. *Meas. Sci. Technol.* (2011). doi:10.1088/0957-0233/22/2/024005
2. Marques Marinho, F. Cellulose and Its Derivatives Use in the Pharmaceutical Compounding Practice. in 141–162 (2013).
3. Alves, L. *et al.* On the role of hydrophobic interactions in cellulose dissolution and regeneration: Colloidal aggregates and molecular solutions. *Colloids Surfaces A Physicochem. Eng. Asp.* **483**, 257–263 (2015).
4. S. Price, W. 2 NMR gradient methods in the study of proteins. *Annu. Reports Sect. 'C' (Physical Chem.* **96**, 3–53 (2000).
5. Price, W. . Applications of pulsed gradient spin-echo NMR diffusion measurements to solution dynamics and organization. *Diffus. Fundam.* **2**, 112.1-112.19 (2005).
6. Tadros, T. F. Principles of Viscoelastic Behavior. in *Rheology of Dispersions* 65–84 (Wiley-VCH Verlag GmbH & Co. KGaA, 2010). doi:10.1002/9783527631568.ch4
7. Pereira, A. *et al.* Cellulose gelation in NaOH solutions is due to cellulose crystallization. *Cellulose* (2018). doi:10.1007/s10570-018-1794-3
8. J., L. P. *et al.* Pollution and Global Health – An Agenda for Prevention. *Environ. Health Perspect.* **126**, 84501 (2018).
9. Wang, S., Lu, A. & Zhang, L. Recent advances in regenerated cellulose materials. *Prog. Polym. Sci.* **53**, 169–206 (2016).
10. Kilpeläinen, I. *et al.* Dissolution of Wood in Ionic Liquids. *J. Agric. Food Chem.* **55**, 9142–9148 (2007).
11. Junior, S., Silva, D., Gabriel, M. & Reali De Oliveira Braga, W. *The Influence of Environmental Concern and Purchase Intent in Buying Green Products.* *Asian Journal of Behavioural Studies* **3**, (2018).

-
12. Vowles, N. S. & Chang, T.-Z. (Donald). Measuring consumer readiness to purchase green products. *J. Cust. Behav.* **17**, 31–47 (2018).
 13. Moon, R. J., Martini, A., Nairn, J., Simonsen, J. & Youngblood, J. Cellulose nanomaterials review: Structure, properties and nanocomposites. *Chemical Society Reviews* (2011). doi:10.1039/c0cs00108b
 14. Medronho, B., Romano, A., Miguel, M. G., Stigsson, L. & Lindman, B. Rationalizing cellulose (in)solubility: Reviewing basic physicochemical aspects and role of hydrophobic interactions. *Cellulose* **19**, 581–587 (2012).
 15. Cao, Y. *et al.* Room temperature ionic liquids (RTILs): A new and versatile platform for cellulose processing and derivatization. *Chem. Eng. J.* **147**, 13–21 (2009).
 16. Isik, M., Sardon, H. & Mecerreyes, D. Ionic liquids and cellulose: Dissolution, chemical modification and preparation of new cellulosic materials. *International Journal of Molecular Sciences* (2014). doi:10.3390/ijms150711922
 17. Kang, H., Liu, R. & Huang, Y. Cellulose-Based Gels. *Macromol. Chem. Phys.* **217**, 1322–1334 (2016).
 18. Martin-Bertelsen, B. *et al.* Revisiting the dissolution of cellulose in NaOH as ‘Seen’ by X-rays. *Polymers (Basel)*. **12**, (2020).
 19. Bengtsson, J., Olsson, C., Hedlund, A., Köhnke, T. & Bialik, E. Understanding the Inhibiting Effect of Small-Molecule Hydrogen Bond Donors on the Solubility of Cellulose in Tetrabutylammonium Acetate/DMSO. *J. Phys. Chem. B* **121**, 11241–11248 (2017).
 20. Siró, I. & Plackett, D. Microfibrillated cellulose and new nanocomposite materials: A review. *Cellulose* (2010). doi:10.1007/s10570-010-9405-y
 21. Vehviläinen, M. Wet-spinning of cellulosic fibres from water-based solution prepared from enzyme-treated pulp. (2015). doi:10.13140/RG.2.1.4372.9129
 22. Klemm, D., Heublein, B., Fink, H. P. & Bohn, A. Cellulose: Fascinating biopolymer

-
- and sustainable raw material. *Angew. Chemie - Int. Ed.* **44**, 3358–3393 (2005).
23. Olabisi, O. *Handbook of thermoplastics. Plastics Engineering* (1997). doi:10.13140/RG.2.1.2068.4881
 24. Olsson, C. & Westm, G. Direct Dissolution of Cellulose: Background, Means and Applications. *Cellul. - Fundam. Asp.* (2013). doi:10.5772/52144
 25. Hsieh, Y. L. Chemical structure and properties of cotton. in *Cotton: Science and Technology* 3–34 (Elsevier Inc., 2006). doi:10.1533/9781845692483.1.3
 26. Tommila, M., Jokilampi, A., Penttinen, R. & Ekholm, E. Cellulose - A Biomaterial with Cell-Guiding Property. in *Cellulose - Medical, Pharmaceutical and Electronic Applications* (2013). doi:10.5772/54436
 27. Budtova, T. & Navard, P. Cellulose in NaOH-water based solvents: a review. *Cellulose* **23**, 5–55 (2016).
 28. Olsson, C. & Westman, G. Direct Dissolution of Cellulose: Background, Means and Applications. *Cellul. Asp.* (2013). doi:10.5772/52144
 29. Young, A. H. Chapter VIII - Fractionation of Starch. in *Food Science and Technology* (eds. WHISTLER, R. O. Y. L., BEMILLER, J. N. & PASCHALL, E. F. B. T.-S. C. and T. (Second E.) 249–283 (Academic Press, 1984). doi:https://doi.org/10.1016/B978-0-12-746270-7.50014-8
 30. Ling, S., Kaplan, D. L. & Buehler, M. J. Nanofibrils in nature and materials engineering. *Nat. Rev. Mater.* **3**, (2018).
 31. Payal, R. S., Bejagam, K. K., Mondal, A. & Balasubramanian, S. Dissolution of cellulose in room temperature ionic liquids: Anion dependence. *J. Phys. Chem. B* (2015). doi:10.1021/jp512240t
 32. Chakrabarty, A. & Teramoto, Y. Recent advances in nanocellulose composites with polymers: A guide for choosing partners and how to incorporate them. *Polymers* **10**, (2018).
-

-
33. French, A. D. Glucose, not cellobiose, is the repeating unit of cellulose and why that is important. *Cellulose* (2017). doi:10.1007/s10570-017-1450-3
 34. Rojas, J. Effect of Polymorphism on the Particle and Compaction Properties of Microcrystalline Cellulose. in *Cellulose - Medical, Pharmaceutical and Electronic Applications* (2013). doi:10.5772/56591
 35. Ahvenainen, P., Kontro, I. & Svedström, K. Comparison of sample crystallinity determination methods by X-ray diffraction for challenging cellulose I materials. *Cellulose* (2016). doi:10.1007/s10570-016-0881-6
 36. O'Sullivan, A. C. Cellulose: The structure slowly unravels. *Cellulose* **4**, 173–207 (1997).
 37. Kontturi, E. Cellulose : dissolution. 1–59 (2015).
 38. Medronho, B. & Lindman, B. Brief overview on cellulose dissolution/regeneration interactions and mechanisms. *Adv. Colloid Interface Sci.* **222**, 502–508 (2015).
 39. Wei, W., Meng, F., Cui, Y., Jiang, M. & Zhou, Z. Room temperature dissolution of cellulose in tetra-butylammonium hydroxide aqueous solvent through adjustment of solvent amphiphilicity. *Cellulose* (2017). doi:10.1007/s10570-016-1113-9
 40. Lindman, B., Karlström, G. & Stigsson, L. On the mechanism of dissolution of cellulose. *J. Mol. Liq.* **156**, 76–81 (2010).
 41. Duarte, H. Desenvolvimento e caracterização de solventes aquosos para a dissolução de celulose: reologia e comportamento de fase. (2014).
 42. Chami Khazraji, A. & Robert, S. Interaction effects between cellulose and water in nanocrystalline and amorphous regions: A novel approach using molecular modeling. *J. Nanomater.* (2013). doi:10.1155/2013/409676
 43. Alves, C. H. Cellulose solutions : Dissolution , regeneration , solution structure and molecular interactions. 144 (2015).
 44. Lindman, B., Medronho, B. & Theliander, H. Editorial : Cellulose dissolution and
-

-
- regeneration : systems and interactions. *Nord. Pulp Pap. Res. J.* **30**, 2–3 (2015).
45. Glasser, W. G. *et al.* About the structure of cellulose: Debating the Lindman hypothesis. *Cellulose* **19**, 589–598 (2012).
 46. Pérez, S. & Mazeau, K. Conformations, Structures, and Morphologies of Celluloses. in *Polysaccharides* (2004). doi:10.1201/9781420030822.ch2
 47. Nagarajan, S., Skillen, N. C., Irvine, J. T. S., Lawton, L. A. & Robertson, P. K. J. Cellulose II as bioethanol feedstock and its advantages over native cellulose. *Renewable and Sustainable Energy Reviews* (2017). doi:10.1016/j.rser.2017.03.118
 48. Alves, L., Medronho, B., Antunes, F. E., Topgaard, D. & Lindman, B. Dissolution state of cellulose in aqueous systems. 1. Alkaline solvents. *Cellulose* **23**, 247–258 (2016).
 49. Lindman, B. & Medronho, B. The subtleties of dissolution and regeneration of cellulose: Breaking and making hydrogen bonds. *BioResources* (2015). doi:10.15376/biores.10.3.3811-3814
 50. Gentile, L. & Olsson, U. Cellulose-solvent interactions from self-diffusion NMR. *Cellulose* **23**, 2753–2758 (2016).
 51. Kihlman, M., Medronho, B. F., Romano, A. L., Germgård, U. & Lindman, B. Cellulose dissolution in an alkali based solvent: Influence of additives and pretreatments. *J. Braz. Chem. Soc.* **24**, 295–303 (2013).
 52. Hagman, J. *et al.* On the dissolution state of cellulose in cold alkali solutions. *Cellulose* **6**, 30199–30204 (2017).
 53. Feng, L. & Chen, Z. lan. Research progress on dissolution and functional modification of cellulose in ionic liquids. *J. Mol. Liq.* **142**, 1–5 (2008).
 54. Walderhaug, H., Söderman, O. & Topgaard, D. Self-diffusion in polymer systems studied by magnetic field-gradient spin-echo NMR methods. *Prog. Nucl. Magn.*
-

-
- Reson. Spectrosc.* **56**, 406–425 (2010).
55. Medronho, B. & Lindman, B. Competing forces during cellulose dissolution: From solvents to mechanisms. *Curr. Opin. Colloid Interface Sci.* **19**, 32–40 (2014).
56. Lindman, B. & Medronho, B. The Subtleties of Dissolution and Regeneration of Cellulose : Breaking and Making Hydrogen Bonds. **10**, 3811–3814 (2015).
57. Murthy, N. S. X-ray Diffraction from Polymers. *Polymer Morphology* 14–36 (2016). doi:doi:10.1002/9781118892756.ch2
58. Yamanobe, T. & Uehara, H. NMR Analysis of Morphology and Structure of Polymers. *Polymer Morphology* 131–150 (2016). doi:doi:10.1002/9781118892756.ch8
59. Behrens, M. A., Holdaway, J. A., Nosrati, P. & Olsson, U. On the dissolution state of cellulose in aqueous tetrabutylammonium hydroxide solutions. *RSC Adv.* **6**, 30199–30204 (2016).
60. Atkins, P. & Paula, J. De. Atkins' Physical chemistry 9th edition. in *Atkins' Physical chemistry 9th edition* (2009). doi:10.1021/ed056pA260.1
61. De Rosa, Claudio and Auriemma, F. *Crystals and Crystallinity in Polymers. Crystals and Crystallinity in Polymers* (John Wiley & Sons, Inc., 2013). doi:10.1002/9781118690444
62. Ghasemi, M., Tsianou, M. & Alexandridis, P. Assessment of solvents for cellulose dissolution. *Bioresour. Technol.* **228**, 330–338 (2017).
63. Söderman, O., Price, W. S., Schönhoff, M. & Topgaard, D. NMR diffusometry applied to liquids. *J. Mol. Liq.* **156**, 38–44 (2010).
64. Miao, J., Sun, H., Yu, Y., Song, X. & Zhang, L. Quaternary ammonium acetate: An efficient ionic liquid for the dissolution and regeneration of cellulose. *RSC Adv.* (2014). doi:10.1039/c4ra06258b
65. Swatloski, R. P., Spear, S. K., Holbrey, J. D. & Rogers, R. D. Dissolution of cellose
-

-
- with ionic liquids. *J. Am. Chem. Soc.* (2002). doi:10.1021/ja025790m
66. Gericke, M., Fardim, P. & Heinze, T. Ionic liquids - Promising but challenging solvents for homogeneous derivatization of cellulose. *Molecules* **17**, 7458–7502 (2012).
67. Schulz, L., Seger, B. & Burchard, W. Structures of cellulose in solution. *Macromol. Chem. Phys.* **201**, 2008–2022 (2000).
68. Singh, P. *et al.* From Cellulose Dissolution and Regeneration to Added Value Applications — Synergism Between Molecular Understanding and Material Development. 1–44 doi:10.5772/61402
69. Bialik, E. *et al.* Ionization of Cellobiose in Aqueous Alkali and the Mechanism of Cellulose Dissolution. *J. Phys. Chem. Lett.* **7**, 5044–5048 (2016).
70. Roy, C., Budtova, T. & Navard, P. Rheological Properties and Gelation of Aqueous Cellulose–NaOH Solutions. *Biomacromolecules* **4**, 259–264 (2003).
71. Hagman, J. *et al.* On the dissolution state of cellulose in cold alkali solutions. *Cellulose* 1–26 (2017). doi:10.1007/s10570-017-1272-3
72. Nosrati, P. On the Gelation of Microcrystalline Cellulose in Alkaline Solutions. (2016).
73. Yao, Y. *et al.* Mechanistic study on the cellulose dissolution in ionic liquids by density functional theory. *Chinese J. Chem. Eng.* **23**, 1894–1906 (2015).
74. Isobe, N., Kimura, S., Wada, M. & Kuga, S. Mechanism of cellulose gelation from aqueous alkali-urea solution. *Carbohydr. Polym.* **89**, 1298–1300 (2012).
75. Weng, L., Zhang, L., Ruan, D., Shi, L. & Xu, J. Thermal Gelation of Cellulose in a NaOH/Thiourea Aqueous Solution. *Langmuir* **20**, 2086–2093 (2004).
76. Gubitosi, M. *et al.* Stable, metastable and unstable cellulose solutions. *R. Soc. Open Sci.* **4**, 1–25 (2017).
-

-
77. Medronho, B. *et al.* Probing cellulose amphiphilicity. *Nord. Pulp Pap. Res. J.* (2015).
 78. Sun, N., Rodríguez, H., Rahman, M. & Rogers, R. D. Where are ionic liquid strategies most suited in the pursuit of chemicals and energy from lignocellulosic biomass? *Chem. Commun.* (2011). doi:10.1039/c0cc03990j
 79. Abe, M., Fukaya, Y. & Ohno, H. Fast and facile dissolution of cellulose with tetrabutylphosphonium hydroxide containing 40 wt% water. *Chem. Commun.* **48**, 1808 (2012).
 80. Gubitosi, M., Duarte, H., Gentile, L., Olsson, U. & Medronho, B. On cellulose dissolution and aggregation in aqueous tetrabutylammonium hydroxide. *Biomacromolecules* **17**, 2873–2881 (2016).
 81. Gentile, L. & Olsson, U. Cellulose–solvent interactions from self-diffusion NMR. *Cellulose* **23**, 2753–2758 (2016).
 82. Wang, Y., Liu, L., Chen, P., Zhang, L. & Lu, A. Cationic hydrophobicity promotes dissolution of cellulose in aqueous basic solution by freezing-thawing. *Phys. Chem. Chem. Phys.* (2018). doi:10.1039/c8cp01268g
 83. Cao, J. *et al.* Cellulose films from the aqueous DMSO/TBAH-system. *Cellulose* **25**, (2018).
 84. Schönhoff, M. NMR studies of sorption and adsorption phenomena in colloidal systems. *Curr. Opin. Colloid Interface Sci.* **18**, 201–213 (2013).
 85. Idström, A. *et al.* On the dissolution of cellulose in tetrabutylammonium acetate/dimethyl sulfoxide: a frustrated solvent. *Cellulose* **24**, 3645–3657 (2017).
 86. Hughes, G. and. *Rheology for Chemists. Rheology for Chemists* (2008). doi:10.1039/9781847558046
 87. Naé, H. N. Introduction to rheology. in *Rheological Properties of Cosmetics and Toiletries* (2017). doi:10.1201/9780203740651
 88. Tabilo-Munizaga, G. & Barbosa-Cánovas, G. V. Rheology for the food industry. *J.*
-

-
- Food Eng.* **67**, 147–156 (2005).
89. Remz, H. M. Nail product rheology. in *Rheological Properties of Cosmetics and Toiletries* 153–222 (2017). doi:10.1201/9780203740651
 90. Franck, A. Understanding rheology of structured fluids. *B. TA instruments* 1–11 (2004).
 91. Strivens, T. A. An introduction to rheology. in *Paint and Surface Coatings* (1999). doi:10.1533/9781855737006.550
 92. Shaw, M. T. *Introduction to Polymer Rheology. Introduction to Polymer Rheology* (2012). doi:10.1002/9781118170229
 93. Mezger, T. G. *Applied rheology : with Joe Flow on Rheology Road.* (2015).
 94. Kaneda, I. *Rheology of biological soft matter: fundamentals and applications.* (2016).
 95. Tadros, T. F. *Rheology of Dispersions: Principles and Applications. Rheology of Dispersions: Principles and Applications* (2010). doi:10.1002/9783527631568
 96. Peng, B. *et al.* Rheological properties of cellulose nanocrystal-polymeric systems. *Cellulose* **25**, 3229–3240 (2018).
 97. Boisly (geb. Obst), M., Kästner, M., Brummund, J. & Ulbricht, V. General aspects of yield stress fluids - Terminology and definition of viscosity. *Appl. Rheol.* **24**, 14578 (2013).
 98. Garvey, C. J., Parker, I. H. & Simon, G. P. On the interpretation of X-ray diffraction powder patterns in terms of the nanostructure of cellulose I fibres. *Macromol. Chem. Phys.* (2005). doi:10.1002/macp.200500008
 99. Topgaard, D. Nuclear Magnetic Resonance studies of water self-diffusion in porous systems. *Phys. Chem. 1, Lund Univ. PhD Thesis*, (2003).
 100. Weingärtner, H. NMR studies of ionic liquids: Structure and dynamics. *Curr. Opin.*
-

-
- Colloid Interface Sci.* **18**, 183–189 (2013).
101. Price, W. S. NMR Diffusometry. in *Modern Magnetic Resonance* (ed. Webb, G. A.) 109–115 (Springer Netherlands, 2006). doi:10.1007/1-4020-3910-7_13
 102. Damodaran, K. *Recent NMR Studies of Ionic Liquids. Annual Reports on NMR Spectroscopy* **88**, (Elsevier Ltd., 2016).
 103. Joseph, P. H. The Basics of NMR. *RIT CIS - Centre of Imaging Science* 14–17 (2011). doi:10.1002/9781118649459.ch2
 104. Kimmich, R. *NMR: Tomography, Diffusometry, Relaxometry. Journal of Chemical Information and Modeling* (1997). doi:10.1017/CBO9781107415324.004
 105. Baur, J. E. Diffusion coefficients. in *Handbook of Electrochemistry* 829–848 (Elsevier, 2007). doi:10.1016/B978-044451958-0.50036-7
 106. Ferreira, T. M., Bernin, D. & Topgaard, D. Chapter Three - NMR Studies of Nonionic Surfactants. in (ed. Webb, G. A. B. T.-A. R. on N. M. R. S.) **79**, 73–127 (Academic Press, 2013).
 107. Momot, K. I. & Kuchel, P. W. PFG NMR diffusion experiments for complex systems. *Concepts Magn. Reson. Part A* **28A**, 249–269 (2006).
 108. Kerssebaum, R. & Salnikov, G. DOSY and Diffusion by NMR. *Topspin - Bruker* 1–32 (2006).
 109. Hrabe, J., Kaur, G. & Guilfoyle, D. N. Principles and limitations of NMR diffusion measurements. *J. Med. Phys.* **32**, 34–42 (2007).
 110. Harmon, J. *et al.* Determination of molecular self-diffusion coefficients using pulsed-field-gradient NMR: An experiment for undergraduate physical chemistry laboratory. *J. Chem. Educ.* (2012). doi:10.1021/ed200471k
 111. Jönsson, B., Wennerström, H., Nilsson, P. G. & Linse, P. Self-diffusion of small molecules in colloidal systems. *Colloid Polym. Sci.* **264**, 77–88 (1986).
-

-
112. Pickup, S. & Blum, F. D. Self-Diffusion of Toluene in Polystyrene Solutions. *Macromolecules* (1989). doi:10.1021/ma00200a025
113. Francis A. Carey, R. J. S. *Advanced Organic Chemistry Part A: Structure and Mechanisms. Advanced Organic Chemistry* (2007). doi:10.1007/978-0-387-44899-2
114. Waggoner, R. A., Blum, F. D. & MacElroy, J. M. D. Dependence of the solvent diffusion coefficient on concentration in polymer solutions. *Macromolecules* (1993). doi:10.1021/ma00077a021
115. Stait-Gardner, T., Willis, S., Yadav, N., Zheng, G. & Price, W. S. NMR Diffusion Measurements of Complex Systems. *J. Basic Princ. Diffus. Theory, Exp. Appl.* (2009).
116. Fatimi, A., Tassin, J. F., Turczyn, R., Axelos, M. A. V. & Weiss, P. Gelation studies of a cellulose-based biohydrogel: The influence of pH, temperature and sterilization. *Acta Biomater.* (2009). doi:10.1016/j.actbio.2009.05.030
117. Kobayashi, K., Kimura, S., Togawa, E. & Wada, M. Crystal transition from Na-cellulose IV to cellulose II monitored using synchrotron X-ray diffraction. *Carbohydr. Polym.* **83**, 483–488 (2011).
118. Muthukumar, M. Shifting Paradigms in Polymer Crystallization. in *Progress in Understanding of Polymer Crystallization* (eds. Reiter, G. & Strobl, G. R.) 1–18 (Springer Berlin Heidelberg, 2007). doi:10.1007/3-540-47307-6_1
119. Takeshita, H., Kanaya, T., Nishida, K. & Kaji, K. Small-angle neutron scattering studies on network structure of transparent and opaque PVA gels. *Phys. B Condens. Matter* **311**, 78–83 (2002).
120. Kanaya, T., Ohkura, M. & Kaji, K. Structure of Poly(vynil alcohol) Gels studied by Wide- and Small-Angle Neutron Scattering. *Macromolecules* **27**, 5609–5615 (1994).
-

-
121. Kanaya, T. *et al.* Gelation Process of Poly(vinyl alcohol) As Studied by Small-Angle Neutron and Light Scattering. *Macromolecules* **28**, 3168–3174 (1995).
 122. Hyon, S.H., Cha, W.I. & Ikada, Y. Preparation of transparent poly(vinyl alcohol) hydrogel. *Polym. Bull.* **22**, 119–122 (1989).
 123. Medronho, B. *et al.* From a new cellulose solvent to the cyclodextrin induced formation of hydrogels. *Colloids Surfaces A Physicochem. Eng. Asp.* **532**, 548–555 (2017).
 124. Bengtsson, J. Evaluating recyclability and suitability of tetrabutylammonium acetate : dimethyl sulfoxide as a solvent for cellulose. (2016).
 125. Lindman, B., Puyal, M. C., Kamenka, N., Brun, B. & Gunnarsson, G. Micelle formation of ionic surfactants. Tracer self-diffusion studies and theoretical calculations for sodium p-octylbenzenesulfonate. *J. Phys. Chem.* **86**, 1702–1711 (1982).
 126. Abe, M., Kuroda, K. & Ohno, H. Maintenance-Free Cellulose Solvents Based on Onium Hydroxides. *ACS Sustain. Chem. Eng.* (2015). doi:10.1021/acssuschemeng.5b00303
 127. Burchard, W. Solubility and solution structure of cellulose derivatives. *Cellulose* (2003). doi:10.1023/A:1025160620576
 128. Huang, Y. B. *et al.* Room-Temperature Dissolution and Mechanistic Investigation of Cellulose in a Tetra-Butylammonium Acetate/Dimethyl Sulfoxide System. *ACS Sustain. Chem. Eng.* (2016). doi:10.1021/acssuschemeng.5b01749
 129. Andanson, J. *et al.* Understanding the Role of Co-solvents in the Dissolution of Cellulose in Ionic Liquids. *Green Chem.* **16**, (2014).
 130. Medronho, B. *et al.* The role of cyclodextrin-tetrabutylammonium complexation on the cellulose dissolution. *Carbohydr. Polym.* **140**, 136–143 (2016).

Appendix A. Pb and graphs

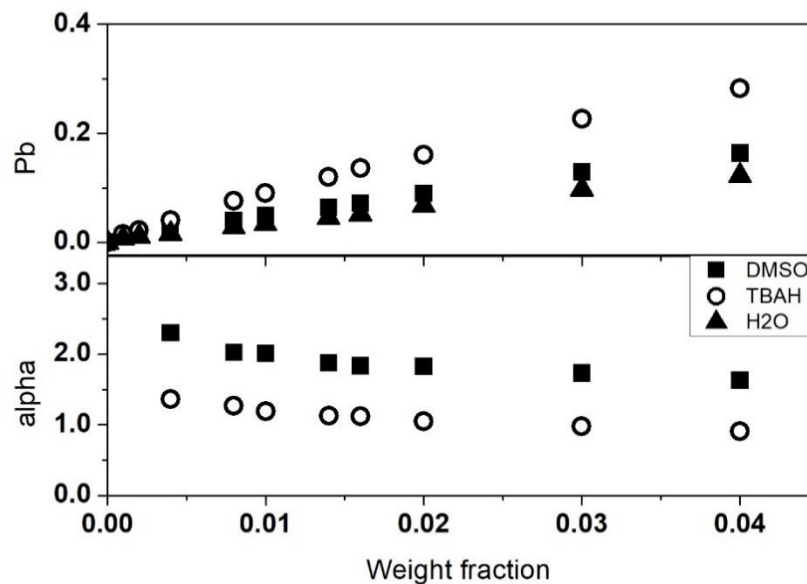


Figure A.1. Fraction of bound molecules of DMSO, TBAH and water as a function of weight fraction (top) and α values of DMSO and TBA⁺ ions as a function of weight fraction (bottom), in a solution of DMSO and TBAH (40%) in a ratio of 1:1.

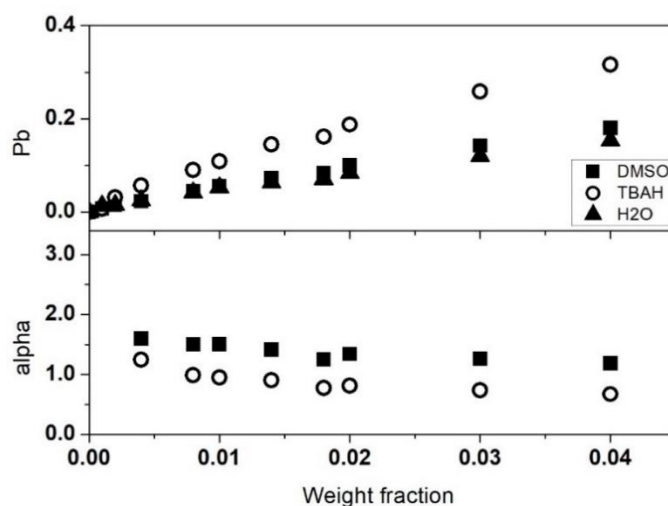


Figure A.2. Fraction of bound molecules of DMSO, TBAH and water as a function of cellulose weight fraction (top) and α values of DMSO and TBA⁺ ions (bottom) as a function of cellulose weight fraction, in a solution of DMSO and TBAH (40%) in a 1:2 ratio.

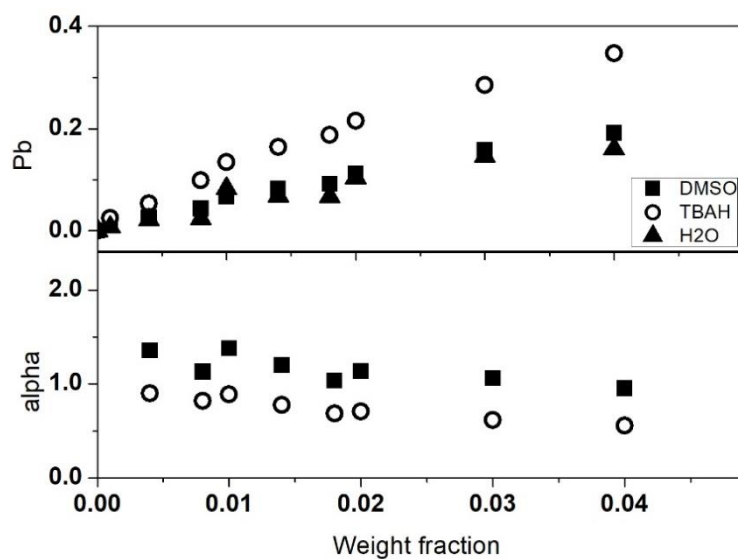


Figure A.3. Fraction of bound molecules of DMSO, TBAH and water as a function of weight fraction (on top) and α values of DMSO and TBA⁺ ions (bottom) as a function of weight fraction, in a solution of DMSO and TBAH (40%) in a 1:3 ratio.

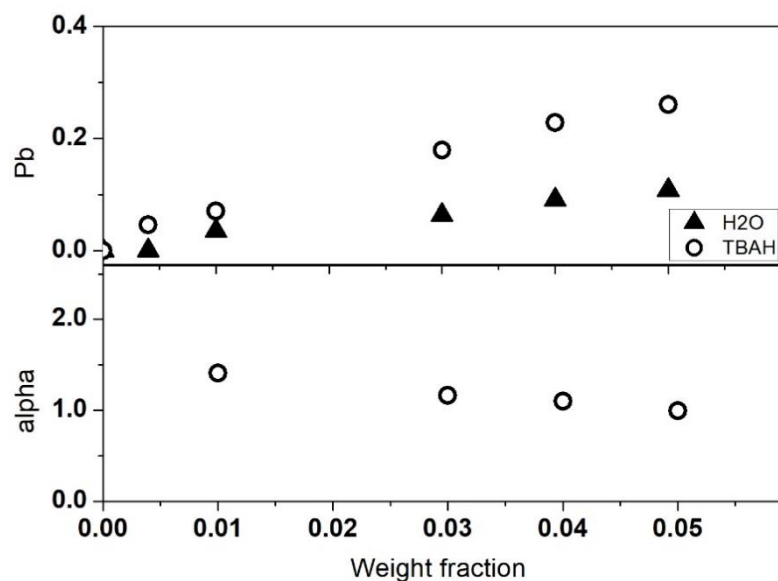


Figure A.4. Fraction of bound molecules of TBAH and water as a function of weight fraction (on top) and α values of TBA⁺ ions as a function of weight fraction, in a solution of TBAH (30%).

Appendix B. Published article


<https://doi.org/10.1007/s10570-018-1794-3>

Cellulose (2018) 25:3205–3210
<https://doi.org/10.1007/s10570-018-1794-3>



COMMUNICATION

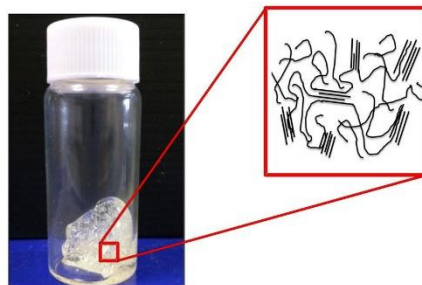
Cellulose gelation in NaOH solutions is due to cellulose crystallization

Ana Pereira · Hugo Duarte · Pegah Nosrati · Marta Gubitosi · Luigi Gentile · Anabela Romano · Bruno Medronho  · Ulf Olsson

Received: 25 January 2018 / Accepted: 11 April 2018 / Published online: 19 April 2018
© Springer Science+Business Media B.V., part of Springer Nature 2018

Abstract Cellulose gelation in 2 M NaOH aqueous solution was followed by time resolved turbidity and rheology measurements. The kinetics of gelation is observed to change from several hours down to few seconds when the temperature is increased from 25 to 30 °C. The increase of turbidity upon gelation demonstrates the formation of larger cellulose aggregates, while wide angle X-ray scattering data confirms the gradual formation of crystalline domains. This suggests that the gelation can be understood as cellulose precipitation/crystallization where an effectively cross linked network and gelation results from that cellulose chains may participate in more than one crystallite.

Graphical Abstract The gelation of cellulose solutions is due to crystallization and precipitation of cellulose.



Keywords Cellulose · Gelation · NaOH · Crystallites, WAXS

Introduction

Cellulose processing for new advanced materials is a rather challenging issue since dissolution is often an initial required step but far from being trivial (Klemm et al. 2005; Medronho and Lindman 2014; Singh et al. 2015). The list of efficient solvent systems is limited, and current discussion is still not unanimous on the relevant solvent key features or interactions that drive

A. Pereira · A. Romano · B. Medronho (✉)
Faculty of Sciences and Technology (MeditBio), Ed. 8,
University of Algarve, Campus de Gambelas,
8005-139 Faro, Portugal
e-mail: bfmedronho@ualg.pt

P. Nosrati · M. Gubitosi · L. Gentile · U. Olsson
Division of Physical Chemistry, Department of
Chemistry, Lund University, P.O. Box 124, 221 00 Lund,
Sweden

H. Duarte
Department of Chemistry “Ugo Schiff”, Università di
Firenze and CSGI, Via della Lastruccia 31, Sesto
Fiorentino, 50019 Florence, Italy

 Springer

dissolution (Glasser et al. 2012; Gubitosi et al. 2017; Idstrom et al. 2017; Liebert 2009; Lindman et al. 2010; Medronho et al. 2012). Nevertheless, once dissolved, the cellulose solutions are typically metastable and thus sensitive to aging or pH and temperature changes, which may induce gelation-regeneration of the cellulose dopes (Isobe et al. 2012; Medronho and Lindman 2015; Roy et al. 2003). Such gelation-regeneration phenomenon is not only interesting from a fundamental point of view but of major importance for the development of, for instance, cellulose-based films or fibers (Yamane et al. 1996). Among the solvent systems available, aqueous NaOH is a common solvent for cellulose dissolution particularly due to the fact that it is inexpensive and considered of low toxicity (Budtova and Navard 2016). Recently, it was observed that microcrystalline cellulose (MCC) can be dispersed in NaOH at concentrations lower than 1 wt% and samples are stable for up to two months at room temperature (Hagman et al. 2017). Generally, the conditions for dissolution in NaOH(aq) must be rigorously controlled: dissolution occurs within a narrow temperature (i.e. sub-zero) and concentration (ca. 1.5–2.5 M) ranges (Alves et al. 2016). The reason for this can be understood from the opposite dependences of the solubility on the NaOH concentration of neutral cellulose and its sodium salts (Gubitosi et al. 2017).

It is well established that the cellulose solution in aqueous alkali stability is strongly temperature dependent. Roy et al., performed time resolved rheological measurements of the linear viscoelastic properties of cellulose solutions in 2.2 M NaOH(aq) in the temperature range 15–35 °C (Roy et al. 2003). It was found that the estimated gelation time, t_{gel} , obtained from the storage and loss moduli crossover, decreased essentially exponentially with increasing temperature. Similar results have been reported by Weng et al. in NaOH/thiourea based system. Nevertheless, the reason for such gelation was not clarified, and has since not yet been fully explained (Budtova and Navard 2016; Roy et al. 2003; Weng et al. 2004). Thus, in order to better understand this gelation phenomenon on the molecular level, wide angle X-ray diffraction experiments at different temperatures have been performed. These experiments are expected to provide insights on the association of cellulose molecules. In addition, time resolved turbidity data and rheology

experiments are presented to further characterize the cellulose aggregation and gelation, respectively.

Materials and methods

Materials

The microcrystalline cellulose, Avicel PH101, Lot: 61113C, Box 00,083, was purchased from Sigma-Aldrich. The sodium hydroxide, 97% pure, anhydrous pellets, was purchased from Merck, Darmstadt, Germany. The water used was purified in-house using a MILLIPORE Milli-Q Gradient A10, Millipore, Molsheim, France.

Sample preparation

A solution of 2.0 M NaOH was prepared as stock solution by dissolving NaOH pellets in Milli-Q water. The stock solution was pre-cooled in an ice bath and MCC was then slowly added to the solution under vigorous stirring using a magnetic stirrer. The dispersion was left stirring in the ice bath until becoming a semi-transparent, homogeneous dispersion (> 5 min). Afterwards, the solution was incubated at – 20 °C for 20 min. Once the sample had undergone the freezing step, it was thaw at room temperature by first letting it stir in an ice bath for 10 min followed by stirring without any temperature control for an additional 20 min. After the final stirring, the samples were ready and kept at room temperature.

Wide-angle X-ray scattering (WAXS)

Wide-angle X-ray scattering measurements were performed using the SAXSLab Ganesha 300XL instrument (SAXSLAB ApS, Skovlunde, Denmark), a pinhole collimated system equipped with a Genix 3D X-ray source (Xenocs SA, Sassenage, France). Data were collected with the detector placed at a sample-to-detector positions that yields to the WAXS region between 0.5 and 2.5 Å⁻¹. The gel sample was sealed in the capillary (1.5 mm diameter) and measured just after preparation and after 9 and 144 h at 45 °C. Note that the gel was not pre-washed. During the experiments the temperature was controlled by an external recirculating water bath with a temperature accuracy of 0.2 °C and kept constant to 25 °C. The two-

dimensional (2D) scattering pattern was recorded using a 2D 300 k Pilatus detector (Dectris Ltd., Baden, Switzerland) and radially averaged using the SAXS-Gui software to obtain $I(q)$. The reciprocal space conversion to real space is obtained by $2\pi/q$. The scattering profile was obtained by subtracting the solvent (data acquired in the same capillary with the same exposure time) and the data was brought to absolute scale using water as a primary standard.

Rheology

Rheological measurements have been carried out using an Anton Paar Physica MCR 301 stress controlled rheometer (Anton Paar, Germany) with direct strain oscillation for real-time strain control equipped with a Couette cylinder geometry (cup diameter: 28.929 mm, bob diameter: 26.673 mm, bob length: 39.997 mm). The temperature was controlled using a water circulator apparatus (± 0.2 °C). To prevent evaporation, an appropriate solvent trap was used. All investigated samples were firstly loaded in the Couette cylinder at 10 °C since the gelation process is rather slow at low temperatures and subsequently the target temperature was set to a higher value, between 25 and 30 °C.

Turbidity measurements

The absorbance of cellulose solutions was measured at 800, 825, and 850 nm on an UV/vis spectrometer (Specorde 200 Plus, Analytic Jena). None of the chemical species in the solution show any absorption at these wavelengths. Hence, the measured absorbance is solely due to scattering and can be used to calculate the turbidity as, $-(1/L)\ln(T)$ where T is the average transmission from the three wavelengths and L is the optical path length of the cuvette.

Results and Discussion

In the present work the alkali system is revisited and the influence of temperature on the gelation kinetics of 4 wt% cellulose in 2 M NaOH(aq) is studied by means of time-resolved dynamic experiments from 25 to 30 °C (Fig. 1). As it can be observed in the insert of Fig. 1, the sample initially behaves as a viscous fluid with the loss modulus G'' higher than the storage

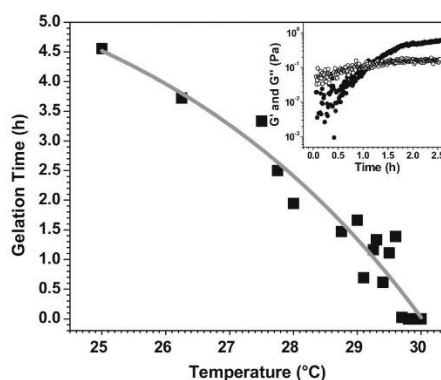


Fig. 1 Gelation time, t_{gel} , of 4 wt% MCC in 2.0 M NaOH as a function of temperature. The solid line is a guide to the eyes. The inset shows an example of the time evolution of G' (full circles) and G'' (empty circles) at 29.5 °C. Qualitative similar profiles are generally observed for all temperatures. The time-resolved oscillatory measurements were performed at a constant angular frequency of 1 rad/s and strain of 0.1% (within the linear viscoelastic regime)

modulus G' . G' evolves much faster than G'' until their crossover is observed (i.e. the gel point, t_{gel} , is defined as the time when $G' = G''$). It is striking that t_{gel} changes from several hours at room temperature to a couple of minutes for temperatures around 30 °C or above. The data in Fig. 1 are consistent with the earlier work of Roy et al., who studied 5 wt% cellulose in 2.2 M NaOH(aq) (Roy et al. 2003).

Recent SAXS measurements revealed that cellulose aggregation increases with increasing temperature, as shown by an increased scattering intensity at lower q values (Hagman et al. 2017). Variations in light scattering can also be followed by turbidity experiments. In Fig. 2a, a time resolved turbidity study is reported where the temperature was alternating between 25 and 45 °C, being changed every 2 h. As it can be seen, the turbidity remains essentially constant when the temperature is 25 °C, while it increases with time at 45 °C. This shows that at 45 °C there is a gradual increase in cellulose aggregation, but no such increase is observed at 25 °C on the time scale of 2 h. The fact that the turbidity and the complex viscosity are retained when lowering the temperature from 45 to 25 °C indicates that the aggregation is irreversible and that at 25 °C the solutions are only kinetically stable.

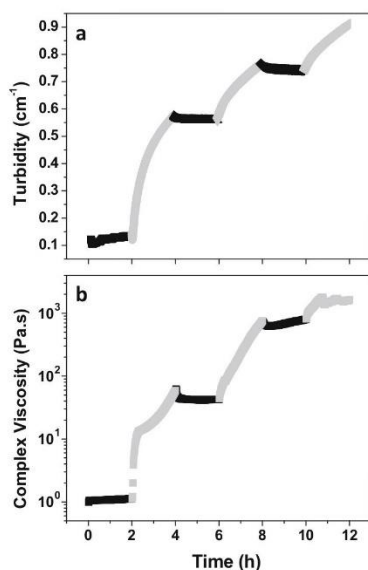


Fig. 2 Turbidity (a) and complex viscosity (b) temperature experiments alternating between 25 (black symbols) and 45 °C (grey symbols) for 4 wt% MCC in NaOH(aq). Samples were kept for 2 h at each temperature before changing to the other temperature

In Fig. 2b, the time evolution of the complex viscosity, following the same temperature cycling as in the turbidity experiments, is presented. As it can be seen, the viscosity data essentially follows the turbidity data (Weng et al. 2004). At 45 °C the viscosity gradually increases with time while it essentially remains constant when the temperature is 25 °C. The data in Figs. 2a and 2b clearly demonstrates (1) the coupling between the sample viscosity and the aggregation state of cellulose, (2) the irreversibility of the aggregation process, and (3) the significant difference in aggregation kinetics between 25 and 45 °C.

The irreversibility is further illustrated in Fig. 3. Here, the evolution of G' and G'' are continuously monitored during a temperature ramp, at a constant heating rate (1 °C/min) and angular frequency of 1 rad/s. During heating from 10 to 25 °C, the sample behaves as a liquid-like solution with $G'' > G'$. At about 26 °C, G' and G'' , crossover and G' increases strongly with increasing temperature. When the temperature is reversed from 40 to 10 °C, only minor

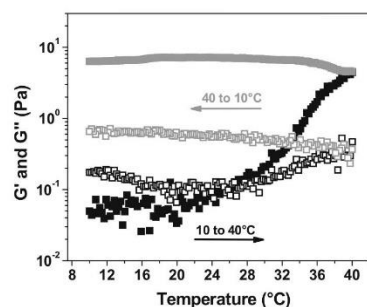


Fig. 3 Temperature sweeps for 4 wt% MCC in NaOH(aq) from 10 to 40 °C (black squares) and from 40 to 10 °C (grey squares). The elastic and viscous moduli are represented by the filled and empty symbols, respectively. The test was performed at a constant frequency of 1 rad/s and strain of 0.1%. The heating and cooling rates were kept constant at 1 °C/min. As can be seen, the viscoelastic parameters at 40 °C values are maintained as the sample is cooled back to 10 °C, demonstrating that the gelation is irreversible

changes are observed in respect to the final stage at 40 °C achieved with the first ramp test.

To further characterize the aggregation of cellulose at elevated temperatures, a sample was stored at 45 °C and WAXS experiments were performed directly after preparation, and also after 9 and 144 h. The solvent subtracted WAXS patterns are presented in Fig. 4a. As can be seen, there is a weak diffraction peak at $q = 1.4 \text{ \AA}^{-1}$ that grows in intensity with time. At longer times, a second peak at $q = 1.55 \text{ \AA}^{-1}$ is also observed. The observed diffraction is attributed to the precipitation of crystalline cellulose, presumably partly as sodium salt due to the high pH. The fact that only one or two diffraction peaks are observed suggests that crystallites are still small. The two reflections can be indexed to the 110 and 020 reflections of Na Cellulose IV crystals or Cellulose II (Kobayashi et al. 2011). The results are consistent with those of Isobe et al. who studied cellulose precipitation from alkali-urea solutions (Isobe, et al., 2012).

Precipitation of cellulose II has been recently suggested to occur in another strong alkaline system, 40 wt% tetrabutylammonium hydroxide (Gubitosi et al. 2016). Cellulose II is a more stable crystalline form compared to native Cellulose I and therefore dissolving Cellulose I (MCC) may result in a super-saturated state with respect to Cellulose II that

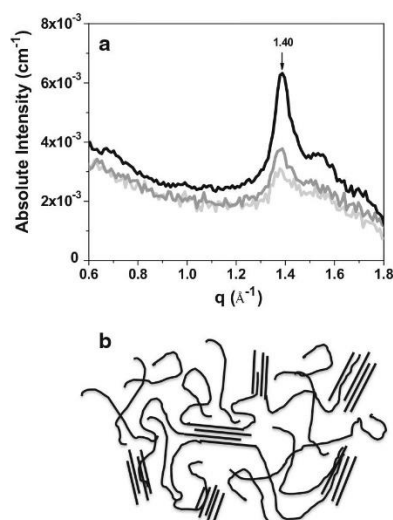


Fig. 4 **a** WAXS-patterns of freshly prepared (light grey line), aged for 9 h (dark grey line) and aged 144 h (black line) 4 wt% of MCC in NaOH(aq) solutions at 45 °C. The arrow highlights the evolution of the main diffraction peak at $q = 1.4 \text{ \AA}^{-1}$. **b** Cartoon illustrating the gel structure obtained from the cellulose crosslinking where the crystallites are suggested to work as junction points

(slowly) precipitates. Thus, it is here suggested that the observed gelation is due to the precipitation and crystallization of cellulose. A cartoon on the hypothetical gel structure is shown in Fig. 4b where cellulose chains may participate in more than one crystallite to form the 3D cross linked network.

Polymer crystallization is a complex process, possibly involving multiple kinetically trapped states (Muthukumar 2007). In the nucleation and growth process, the long chain molecules may be part in more than one crystallite. The crystallites may thus compete for the same molecule and, moreover, such crystallites can act as effective cross-linkers. Gelation is in fact a general feature of polymer crystallization and this has been extensively studied for e.g. poly(vinyl alcohol), PVA (Hyon et al. 1989; Kanaya et al. 1994; Kanaya et al. 2002; Ohkura et al. 1992).

Conclusions

Cellulose gelation in 2 M NaOH(aq) has been studied by time resolved rheology, turbidity and wide angle X-ray scattering. We find that the gelation kinetics is strongly temperature dependent, increasing rapidly with increasing temperature. Wide angle X-ray scattering data reveals the formation of crystalline domains, as the sample gels, and we conclude that the gelation is due to the crystallization and precipitation of cellulose. We also note that this kind of gelation is a common feature of polymer crystallization from solution.

Acknowledgments This work was supported by Nils and Dorthi Troëdssons Foundation, The Swedish Research Council, the Swedish Research Council Formas, and the Portuguese Foundation for Science and Technology (FCT) through project PTDC/AGR-TEC/4814/2014 and researcher grant IF/01005/2014. Ana Pereira acknowledges the support from the ERASMUS + mobility program. UO thanks Masayuki Imai for stimulating discussions.

Compliance with ethical standards

Conflict of interest The authors declare that they have no conflict of interest.

References

- Alves L, Medronho B, Antunes FE, Topgaard D, Lindman B (2016) Dissolution state of cellulose in aqueous systems. 1. Alkaline solvents. *Cellulose* 23(1):247–258
- Budtova T, Navard P (2016) Cellulose in NaOH-water based solvents: a review. *Cellulose* 23(1):5–55
- Glasser WG, Atalla RH, Blackwell J, Brown RM, Burchard W, French AD, Klemm DO, Nishiyama Y (2012) About the structure of cellulose: debating the Lindman hypothesis. *Cellulose* 19(3):589–598
- Gubitosi M, Duarte H, Gentile L, Olsson U, Medronho B (2016) On cellulose dissolution and aggregation in aqueous tetrabutylammonium hydroxide. *Biomacromol* 17(9):2873–2881
- Gubitosi M, Nosrati P, Hamid MK, Kuczera S, Behrens MA, Johansson EG, Olsson U (2017) Stable, metastable and unstable cellulose solutions. *R Soc Open Sci* 4(8):170487–170497
- Hagman J, Gentile L, Jessen CM, Behrens M, Bergqvist KE, Olsson U (2017) On the dissolution state of cellulose in cold alkali solutions. *Cellulose* 24(5):2003–2015
- Hyon SH, Cha WI, Ikada Y (1989) Preparation of Transparent Polyvinyl-Alcohol Hydrogel. *Polym Bull* 22(2):119–122
- Idstrom A, Gentile L, Gubitosi M, Olsson C, Stenqvist B, Lund M, Bergqvist KE, Olsson U, Kohnke T, Bialik E (2017) On the dissolution of cellulose in tetrabutylammonium acetate/

- dimethyl sulfoxide: a frustrated solvent. *Cellulose* 24(9):3645–3657
- Isobe N, Kimura S, Wada M, Kuga S (2012) Mechanism of cellulose gelation from aqueous alkali-urea solution. *Carbohydr Polym* 89(4):1298–1300
- Kanaya T, Ohkura M, Kaji K, Furusaka M, Misawa M (1994) Structure of poly(vinyl alcohol) gels studied by wide-angle and small-angle neutron-scattering. *Macromolecules* 27(20):5609–5615
- Kanaya T, Takahashi N, Nishida K, Kaji K, Seto H, Nagao M, Kawabata Y, Takeda T (2002) Neutron spin echo studies on poly (vinyl alcohol) gel in a mixture of dimethyl sulfoxide and water. *J Neutron Res* 10:149–153
- Klemm D, Heublein B, Fink HP, Bohn A (2005) Cellulose: fascinating biopolymer and sustainable raw material. *Angew Chem Int Ed* 44(22):3358–3393
- Kobayashi K, Kimura S, Togawa E, Wada M (2011) Crystal transition from Na-cellulose IV to cellulose II monitored using synchrotron X-ray diffraction. *Carbohydr Polym* 83(2):483–488
- Liebert T (2009) Cellulose Solvents: For Analysis, Shaping and Chemical Modification. In *Cellulose solvents: for analysis, shaping and chemical modification* (Vol 1033, pp 3–54)
- Lindman B, Karlström G, Stigsson L (2010) On the mechanism of dissolution of cellulose. *J Mol Liq* 156(1):76–81
- Medronho B, Lindman B (2014) Competing forces during cellulose dissolution: From solvents to mechanisms. *Curr Opin Colloid Interface Sci* 19(1):32–40
- Medronho B, Lindman B (2015) Brief overview on cellulose dissolution/regeneration interactions and mechanisms. *Adv Coll Interface Sci* 222:502–508
- Medronho B, Romano A, Miguel MG, Stigsson L, Lindman B (2012) Rationalizing cellulose (in)solubility: reviewing basic physicochemical aspects and role of hydrophobic interactions. *Cellulose* 19(3):581–587
- Muthukumar M (2007) Shifting paradigms in polymer crystallization. in progress in understanding polymer crystallization. In: Reiter G, Strobl GR (eds) *Lecture notes in physics*; Springer Berlin Heidelberg: Berlin, Heidelberg, Vol 714, pp 1–18
- Ohkura M, Kanaya T, Kaji K (1992) Gels of poly(vinyl alcohol) from dimethyl-sulfoxide water solutions. *Polymer* 33(17):3686–3690
- Roy C, Budtova T, Navard P (2003) Rheological properties and gelation of aqueous cellulose-NaOH solutions. *Biomacromol* 4(2):259–264
- Singh P, Duarte H, Alves L, Antunes F, Le Moigne N, Dormanns J, Duchemin B, Staiger MP, Medronho M (2015) From cellulose dissolution and regeneration to added value applications—synergism between molecular understanding and material development, cellulose—fundamental aspects and current trends. Dr. Matheus Poletto (ed) *InTech*, <https://doi.org/10.5772/61402>
- Weng LH, Zhang LN, Ruan D, Shi LH, Xu J (2004) Thermal gelation of cellulose in a NaOH/thiourea aqueous solution. *Langmuir* 20(6):2086–2093
- Yamane C, Mori M, Saito M, Okajima K (1996) Structures and mechanical properties of cellulose filament spun from cellulose/aqueous NaOH solution system. *Polym J* 28(12):1039–1047